MOLECULAR AND CELLULAR BIOLOGY, Apr. 2010, p. 1783–1799 Vol. 30, No. 7
0270-7306/10/$12.00 doi:10.1128/MCB.01003-09

Establishment of Extracellular Signal-Regulated Kinase 1/2 Bistability and Sustained Activation through Sprouty 2 and Its Relevance for Epithelial Function▽

Weimin Liu,[1] Kavita Tundwal,[1] Qiaoling Liang,[1] Nicholas Goplen,[1] Sadee Rozario,[1] Nayeem Quayum,[3] Magdalena Gorska,[1] Sally Wenzel,[4] Silvana Balzar,[4] and Rafeul Alam[1,2]*

Division of Allergy and Immunology, Department of Medicine, National Jewish Health, Denver, Colorado[1]; University of Colorado Denver Health Sciences Center, Denver, Colorado[2]; Lerner Research Institute, Department of Stem Cell and Regenerative Medicine Cleveland Clinic, Cleveland, Ohio[3]; and University of Pittsburgh, Department of Medicine, Pittsburgh, Pennsylvania[4]

Received 29 July 2009/Returned for modification 30 September 2009/Accepted 19 January 2010

Our objective was to establish an experimental model of a self-sustained and bistable extracellular signal-regulated kinase 1/2 (ERK1/2) signaling process. A single stimulation of cells with cytokines causes rapid ERK1/2 activation, which returns to baseline in 4 h. Repeated stimulation leads to sustained activation of ERK1/2 but not Jun N-terminal protein kinase (JNK), p38, or STAT6. The ERK1/2 activation lasts for 3 to 7 days and depends upon a positive-feedback mechanism involving Sprouty 2. Overexpression of Sprouty 2 induces, and its genetic deletion abrogates, ERK1/2 bistability. Sprouty 2 directly activates Fyn kinase, which then induces ERK1/2 activation. A genome-wide microarray analysis shows that the bistable phospho-ERK1/2 (pERK1/2) does not induce a high level of gene transcription. This is due to its nuclear exclusion and compartmentalization to Rab5$^+$ endosomes. Cells with sustained endosomal pERK1/2 manifest resistance against growth factor withdrawal-induced cell death. They are primed for heightened cytokine production. Epithelial cells from cases of human asthma and from a mouse model of chronic asthma manifest increased pERK1/2, which is associated with Rab5$^+$ endosomes. The increase in pERK1/2 was associated with a simultaneous increase in Sprouty 2 expression in these tissues. Thus, we have developed a cellular model of sustained ERK1/2 activation, which may provide a mechanistic understanding of self-sustained biological processes in chronic illnesses such as asthma.

An adaptive response of cells to environmental cues is a fundamental biological process that allows optimization of growth, function, and survival. Cells that are unable to adapt to changing environmental cues are unlikely to survive. One of the important elements of this adaptive response is the formation of a "cellular memory" that leads to a programmatic change in the cellular response. Hysteresis, a property of some biochemical systems, is well suited to respond to environmental changes. In physics, hysteresis indicates the history dependence of physical systems (J. Sethna, What is hysteresis? [http://www.lassp.cornell.edu/sethna/hysteresis/WhatIsHysteresis.html]). Systems that display hysteresis can toggle between two alternative stable steady states. This is known as system bistability (18). A bistable system can exist in three states: an "on" state, an "off" state, and an unstable intermediate state. Early examples of biological bistable systems include the lambda phage lysis-lysogeny switch and the hysteretic lac repressor system (55). Lisman in 1985 first suggested that a bistable system could serve as a self-sustaining biochemical memory (29). Bistability arises from a positive-feedback loop or a mutually inhibitory, double-negative-feedback loop (10, 33).

We are interested in exploring bistability in the extracellular signal-regulated kinase 1/2 (ERK1/2) signaling module. Bistability in ERK1/2 has been demonstrated in frog oocytes (53) and in mammalian cells (28). Recent studies have demonstrated bistability in the Sos (5) and Ras (20, 44) signaling modules, which are upstream activators of ERK1/2. In this study we asked the following questions. Does ERK1/2 manifest bistability in human cells? What type of stimulation is needed to induce bistability? What is the mechanism of bistability? How long does bistability persist? What is the biological relevance of ERK1/2 bistability?

MATERIALS AND METHODS

Cell culture and Western blotting. Human primary small airway epithelial cells (SAEC; Cambrex, Inc., East Rutherford, NJ) were cultured with basal serum-free medium (SABM) containing SingleQuot growth supplement. BEAS-2B epithelial cells were grown in bronchial epithelial cell basal medium (BEBM; Lonza) with the addition of the growth factor-enriched supplement bronchial epithelial cell growth medium (BEGM; Cambrex, Inc., East Rutherford, NJ), and the medium was changed every 3 days. The human airway epithelial cell line A549, the human airway fibroblast cell line IMR-90, and the Src family kinase-deficient fibroblast cell line SYF were maintained in Dulbecco's modified Eagle medium (DMEM) containing 10% fetal bovine serum (FBS). The PC12 cell line (ATCC) was cultured in DMEM with 5% horse serum and 10% FBS. Before stimulation, cells were trypsinized and then plated at 4×10^4/ml in a 6-well tissue culture plate. A sample of mouse embryonic fibroblasts with a null mutation for Sprouty 2 was a generous gift from Ben Yu, University of California, San Diego, La Jolla, CA. Epithelial cells and fibroblasts were stimulated with cytokines, growth factors, and inhibitors (epidermal growth factor [EGF], 100 ng/ml; eotaxin, 10 ng/ml; nerve growth factor [NGF], 50 ng/ml; interleukin-4 [IL-4], 10 ng/ml; IL-13, 10 ng/ml; PP2, 10 μM; PD98059, 10 μM). The whole-cell lysate was extracted with radioimmunoprecipitation assay (RIPA) buffer, subjected to 8% SDS-PAGE, and then transferred to a Hybond-P polyvinylidene difluoride

* Corresponding author. Mailing address: Division of Allergy and Immunology, Department of Medicine, National Jewish Health, 1400 Jackson Street, Denver, CO 80206. Phone: (303) 398-1656. Fax: (303) 270-2180. E-mail: alamr@njhealth.org.

▽ Published ahead of print on 1 February 2010.

(PVDF) membrane (Amersham Biosciences). The membrane was blocked with 5% bovine serum albumin (BSA) in 50 mM Tris, 0.15 M NaCl, and 0.015% Tween 20 (TBS-T), immunoblotted with a mouse monoclonal anti-phospho-ERK1/2 (anti-pERK1/2) antibody (Santa Cruz Biotechnology, Santa Cruz, CA), and then incubated with a horseradish peroxidase (HRP)-conjugated anti-mouse IgG (Sigma) antibody. After extensive washing with TBS-T, enhanced chemiluminescence (ECL; Amersham) was added and the membrane was subjected to autoradiography. Even loading of the gel was ascertained by reprobing the membrane with anti-ERK1/2, antiactin, or other appropriate antibodies.

Immunofluorescent staining (IFS). BEAS-2B cells were seeded on sterilized cover slides. After stimulation with IL-13, cells on cover slides were fixed in 4% paraformaldehyde for 20 min at room temperature, incubated with 0.05% saponin for 10 min, blocked with 10% goat serum with 0.05% saponin in phosphate-buffered saline (PBS), and immunostained with the following primary antibodies overnight at 4°C: mouse anti-phospho-ERK1/2 (Cell Signaling, Inc.) or isotype control IgG2a; rabbit polyclonal antibodies against Rab4, Rab5, Rab7, Rab13 (Santa Cruz Biotechnology, Santa Cruz, CA), Rab11 (Zymed), or GM130 (against the Golgi apparatus; Cell Signaling, Inc.); or control rabbit IgG. Mitotracker was used for mitochondrial staining in accordance with the manufacturer's instructions. After a washing, the slides were incubated with a labeled secondary antibody in darkness for 1 h, washed with 0.05% saponin in PBS 3 times, rinsed with PBS, and mounted. The slides were viewed under an epifluorescence microscope (Nikon; Eclipse TE-2000 U microscope with a Coolsnap HQ camera, an automated station, and a *z*-axis motor linked to a personal computer [PC] that is equipped with the Metamorph software, v.6.2 [Molecular Devices, San Diego, CA]). For morphometric and comparative analyses, pictures were taken with an appropriate objective (see the Fig. 9 legend) and the same exposure time.

Quantitative real-time PCR for cytokines. BEAS-2B cells were trypsinized and then plated at 1×10^6/ml in a 60-mm tissue culture plate. Before stimulation, cells were treated with dimethyl sulfoxide (DMSO) or the MEK inhibitor PD98059 (20 nM) for 30 min and then stimulated with IL-13 and tumor necrosis factor alpha (TNF-α). Total cellular RNA was extracted using Trizol reagent (Invitrogen) according to the manufacturer's protocol; the RNA pellet was dissolved in RNase-free water and stored at −80°C until used. RNA was immediately converted to cDNA. A portion (2 μg) of the RNA was converted to cDNA using the first-strand cDNA synthesis kit for reverse transcription-PCR (RT-PCR) as directed by the manufacturer (Invitrogen) in a final volume of 20 μl. The resulting cDNA was stored at −20°C. After the reverse transcription reaction, the first-strand cDNA was then diluted 1:5, and 5 μl of reaction mixture was used in each subsequent PCR. For the real-time PCR, 5 μl of cDNA was used with SYBR green and PCR was performed on an ABI 7000 sequence detection system (Applied Biosystems) according to the manufacturer's protocol. The real-time PCR conditions were as follows: for reverse transcription, incubation at 50°C for 50 min; for PCR, 95° for 10 min; for cycling, 95°C for 0.15 min, 60°C for 1 min, and 72°C for 1 min for 40 cycles.

The PCR primers were as follows: eotaxin 3 forward, TGCTTCCAATACAG CCACAA, and reverse, GAGCAGCTGTTACTGGTGAA; RANTES forward, AGCCCTCGCTGTCATCCTCATT, and reverse, TTGCCACTGGTGTAGAA ATACT; matrix metalloproteinase 9 (MMP9) forward, CGAACTTTGACAGC GACAAG, and reverse, TTCAGGGCGAGGACCATAGA; SCF forward, CC AGGCTCTTTACTCCTGGCT, and reverse, CTGCCCTTGTAAGACTTG GCT; IL-13 forward, TACTCGTTGGCTGAGAGCTG, and reverse, GAGTG TGTTTGTCACCGTTG; TSLP forward, ACCTTCAATCCCACCGCCGGCT, and reverse, GGCAGCCTTAGTTTTCATGGCGA; CCL20 forward, CACAG ACCGTATTCTTCATCCTAAATTTATTG, and reverse, CCCCAGCAAGGT TCTTTCTGTTCTTGGGCTATTGCC; Bcl2 forward, GTGGAGGAGCTCTT CAGGGA, and reverse, AGGCACCCAGGGTGATGCAA; Bax forward, CA CCAGCTCTGAGCAGATC, and reverse, GCTGCCACTCGGAAAAAG; Bim forward, TGGCAAAGCAACCTTCTGATG, and reverse, GCAGGCTGCAAT TGTCTACCT; FOXO3a forward, CTGTCTCCATGGACAATAG, and reverse GCTGGCTTGTTCTCTTGGAT; BID forward, GGCAACCGCAGCAGC CAC, and reverse, TCAGTCCATCCCATTTCT; β-actin forward, CCCTGGA GAAGAGCTACGA, and reverse, TAAAGCCATGCCAATCTCAT. After PCR, the relative expression of each gene was normalized to β-actin to give a relative expression level.

Thymidine incorporation assay. BEAS-2B cells were seeded at 5×10^2 per well in a 96-well plate in triplicate for each group. After repeated stimulation with IL-13 for 3 days, cells were incubated with 1 μCi/μl of [^{3}H]thymidine in 200 μl of medium per well overnight and harvested for thymidine incorporation.

Plasmid construction and transfection. BEAS-2B cells were seeded at 5×10^4/ml in a 6-well plate and transfected with pCGN-sprouty 2 (kindly provided by D. Bar-Sagi, State University of New York at Stony Brook) using Lipofectamine 2000 (Invitrogen) according to the manufacturer's instructions following IL-13 stimulation. After 48 h, overexpression of Sprouty 2 was examined by Western blotting. The Y55F mutant of Sprouty 2 was constructed by site-directed mutagenesis (14). For expression of the recombinant protein, human Sprouty 2 cDNA was isolated from pCGN-sprouty 2 and cloned into the EcoRI/XhoI sites of the pGEX-5x-1 vector (Amersham). The open reading frame was confirmed by sequencing. Glutathione *S*-transferase (GST) fusion proteins were produced and purified according to the method described previously (14) and stored at −80°C.

Sprouty 2 knockdown using siRNA. BEAS-2B cells were plated at 3×10^5/ml in a 6-well plate. Following IL-13 stimulation Sprouty 2 was knocked down with small interfering RNA (siRNA; 20 nm) using the Smart pool (Dharmacon) by electroporation (Amaxa) according to the manufacturer's protocol. Briefly, after stimulation with IL-13, cells were washed, trypsinized, and then suspended at 1×10^6/ml in 400 μl of a mixture of supplement and Nucleofector containing 20 nM Sprouty 2 siRNA. Cells were incubated for 48 h after electroporation before lysis for Western blotting.

In vitro kinase assay. Fyn and ERK1/2 were immunoprecipitated from the whole-cell lysate or lung tissue using 2 μg of anti-Fyn and anti-ERK1/2 antibodies (Santa Cruz Biotechnology, Inc.) and washed three times with lysis buffer and once with kinase buffer (20 mM Tris, pH 7.4, 20 mM NaCl, 1 mM dithiothreitol, and 10 mM $MgCl_2$). The kinase activity of Fyn was determined by measuring the phosphorylation of enolase as a substrate in the presence of recombinant GST or GST-Sprouty 2. The kinase activity of ERK1/2 was determined by measuring the phosphorylation of myelin basic protein. The washed immunoprecipitates were incubated in 40 μl of kinase buffer containing 10 μCi of [γ-^{32}P]ATP at 30°C for 30 min. The samples were resolved by SDS-PAGE and transferred to a nitrocellulose membrane, and detection was accomplished by autoradiography. The membranes were then Western blotted for the respective kinases.

GeneChip microarray experiments and statistical analysis. Isolated RNA was submitted to the University of Colorado Microarray Core Facility for GeneChip analysis using the Affymetrix GeneChip Human Gene 1.0 ST array. The chip comprises more than 22,000 probe sets and 500,000 distinct oligonucleotide features and analyzes the expression levels of 18,400 transcripts and variants, including 14,500 well-characterized human genes. Signal intensity values from the microarray were normalized using the MAS5.0 algorithm. Following a three-step filtering process (to exclude Affymetrix control probe sets, genes with an "absent" call in all samples, and dormant genes with the least moderate variation), principal component analysis (PCA) was conducted to identify sample distribution. Finally, using analysis of variance (ANOVA) (with 10% false-discovery rate [FDR] correction), differentially expressed genes were identified among different sample groups from the filtered data. The PCA and ANOVA analysis were conducted using the Partek GS environment. The difference in the gene expression levels was determined by the Student *t* test ($P \leq 0.05$).

Cell survival assay. BEAS-2B cells were seeded in a six-well plate at 5×10^4 per well and stimulated with IL-13 (10 ng/ml/hour/day) at different time points (no stimulation, days 1 and 3, and day 3 only). Cells were washed on day 4, cultured with BEBM without BEGM, trypsinized, and counted after being stained with propidium iodide and trypan blue at 72 h, 120 h, and 168 h. In select experiments cells were further stained with annexin V and analyzed by flow cytometry.

Rab4a and Rab5a knockdown and survival assay. BEAS-2B cells were seeded in a six-well plate at 5×10^5 cells per well and stimulated with IL-13 (10 ng/ml) for 1 h per day for 3 days and then transfected with Rab4a or Rab5a siRNA on day 4. A nontargeting siRNA that was directed against luciferase was used as a control (Dharmacon; siGENOME SMARTpool). Forty-eight hours later cells were divided into two aliquots. One aliquot was lysed with RIPA buffer for Western blotting to examine Rab4, Rab5, and pERK expression. Another aliquot of cells was cultured in the basic medium BEBM without growth factor-rich BEGM (Lonza). At the conclusion the cells were trypsinized, washed, and stained with propidium iodide.

Immunostaining of airway tissue from the mouse model of experimental asthma and human asthma. The animal and human asthma biopsy protocols were approved by the IACUC and Institutional Review Board (IRB). The immunization and allergen exposure protocol for mouse studies was the same as described previously (30). Immunofluorescent staining of the lung sections for pERK1/2 and Rab5 is described in the previous section.

RESULTS

Establishing ERK1/2 bistability and sustained activation. To establish bistability in the ERK1/2 signaling module, we

used a number of human cell lines: primary airway epithelial cells, BEAS-2B and A549 epithelial cell lines, and the lung fibroblast cell line IMR-90. To induce ERK1/2 activation, we used representative cytokines IL-4 and IL-13, the chemokine eotaxin, and the growth factor EGF. However, for most studies we used IL-13, which activates both epithelial cells and fibroblasts and plays an important role in Th2-type inflammatory diseases (51). In preliminary experiments we examined the basal phosphorylation profile of ERK1/2 without stimulation over 6 days. Human primary small airway epithelial cells (SAEC) were cultured and lysed on day 1 through day 6, separately. We didn't detect any fluctuation of ERK1/2 phosphorylation by Western blotting (Fig. 1A). To examine the kinetics of ERK1/2 phosphorylation following IL-13 stimulation, we stimulated cells for 0, 0.5, 1, 2, 3, and 4 h and lysed them immediately for Western blotting. ERK1/2 phosphorylation increased significantly at 30 min, was sustained for 3 h, and returned to baseline in 4 h (Fig. 1B). We reasoned that repeated exposure, as opposed to a single exposure to a stimulus, is more likely to require cellular adaptation and induce bistability. To test this hypothesis, we stimulated BEAS-2B epithelial cells with IL-4, IL-13, eotaxin, and EGF for 1 h per day for 3 consecutive days. Then the cells were rested for the next 3 days and lysed on day 6. One sample of nonstimulated cells was stimulated on day 6 as a positive control. Western blotting showed strong phosphorylation of ERK1/2 upon acute stimulation of cells with the cytokines on day 6. Surprisingly, a similar level of ERK1/2 phosphorylation was observed in cells that were stimulated only for the first 3 days and then rested for the last 3 days (Fig. 1C and D). The results suggest that ERK1/2 behaves as a bistable system and that 3 days of repeated stimulation induces a sustained phosphorylation state of ERK1/2. Similar results were obtained when SAEC, the lung fibroblast cell line IMR-90, and the airway epithelial cell line A549 were studied instead of BEAS-2B (Fig. 1E). We also applied stimulation on alternate days, which worked equally well (Fig. 1F). A minimum of three stimulations is required, as 2 days of stimulation did not induce ERK1/2 bistability. In order to define the duration of this sustained ERK1/2 phosphorylation, we treated cells with IL-13 for 3 days and studied ERK1/2 phosphorylation on different days after resting the cells in the culture medium. ERK1/2 phosphorylation was detected on day 6, decreased by day 9, and totally disappeared by day 12 (Fig. 1G). A similar persistence of pERK1/2 was observed when cells were stimulated for 4 days in a row and assayed for pERK1/2 on day 10 (Fig. 1H).

We asked if repeated IL-13 stimulation induced sustained phosphorylation of Jun N-terminal protein kinase 1/2 (JNK1/2) and p38, the two other major mitogen-activated protein kinase (MAPK) signaling pathways, and STAT6. Phosphorylation of STAT6 and JNK was detected after acute stimulation on day 6 (Fig. 1I). However, unlike what was found for ERK1/2, the phosphorylation of these signaling molecules after repeated IL-13 stimulation was not sustained on day 6. IL-13 failed to induce p38 phosphorylation in this cell line. The results suggest that among the IL-13-activated major signaling molecules ERK1/2 uniquely manifests bistability in our experimental model and that its sustained activation can be induced by repeated stimulation with cytokines, growth factors, and chemokines in multiple human cell types.

Role of Sprouty 2 in ERK1/2 bistability. Studies were next undertaken to understand the mechanism for self-sustained ERK1/2 phosphorylation induced by repeated IL-13 stimulation. First we examined two ERK1/2-specific cytosolic phosphatases: DUSP6 (MKP3) and DUSP3 (VHR). Both these phosphatases were induced by single and repeated stimulations (Fig. 2A), so this could not explain sustained ERK1/2 phosphorylation. We also examined Cbl, an E3 ubiquitin ligase that is known to downregulate receptor-mediated signaling processes (39). The expression of Cbl was modestly inhibited in both acute- and repeated-stimulation models. Previous studies suggest that Sprouty proteins inhibit ERK1/2 activation by the fibroblast growth factor (FGF) receptor tyrosine kinase (3, 15). On the other hand the EGF receptor-mediated activation of ERK1/2 has been shown to be both enhanced (9, 41, 42, 52) and inhibited (25), depending upon the experimental model used. We examined the role of Sprouty 2, the most frequently studied Sprouty isoform, in our sustained ERK1/2 phosphorylation model. We observed a progressive increase in sustained Sprouty 2 expression in the repeated-stimulation model (Fig. 2B). To determine if Sprouty 2 induction was ERK1/2 dependent, we treated cells with the MEK inhibitor PD98059 from day 4 to day 6 following IL-13 stimulation on days 1 to 3. ERK1/2 phosphorylation and Sprouty 2 expression were decreased in the presence of PD98059 (Fig. 2C). Sprouty 2 undergoes phosphorylation at different sites. Mnk1-mediated phosphorylation of Sprouty 2 promotes its stability (6). We observed increased activating phosphorylation of Mnk1 in our experimental model (Fig. 2D). Since we observed that increased Sprouty 2 expression was associated with sustained ERK1/2 phosphorylation, we asked if overexpression of Sprouty 2 alone would induce ERK1/2 phosphorylation. To determine this, we transfected cells with a Sprouty 2 expression plasmid at low (0.3-μg/ml) and high (1-μg/ml) concentrations. The cells were then stimulated with IL-13 as before. We observed a basal increase in ERK1/2 phosphorylation on day 6 in cells treated with the low dose of the Sprouty 2 expression vector (Fig. 2E). Repeated stimulation with IL-13 did not significantly alter this expression level. In contrast, a high level Sprouty 2 expression inhibited sustained ERK1/2 phosphorylation in the repeated-stimulation model. Our results provide a dose-based explanation for some of the contradictory reports on the effect of Sprouty 2 on ERK1/2 phosphorylation.

To better understand the function of Sprouty 2 in sustained ERK1/2 phosphorylation, we conducted experiments with epithelial cells in which Sprouty 2 expression was knocked down and mouse embryonic fibroblasts that are homozygous for a Sprouty 2 null mutation (24). We used siRNA to inhibit the expression of Sprouty 2 in BEAS-2B cells. Reduced expression of Sprouty 2 in the knockdown epithelial cells (Fig. 2F and G) and the absence of Sprouty 2 in the knockout fibroblasts (Fig. 2H) abrogated the sustained phosphorylation of ERK1/2 in our experimental model. This result establishes an essential role for Sprouty 2 in establishing ERK1/2 bistability and sustained phosphorylation in our model.

Role of Src family kinases. The Src family kinases frequently function upstream of the ERK1/2 signaling module in various receptor signaling pathways. To elucidate the role of Src kinases in IL-13-stimulated ERK1/2 activation and Sprouty 2 expression, we treated cells with the Src family kinase inhibitor

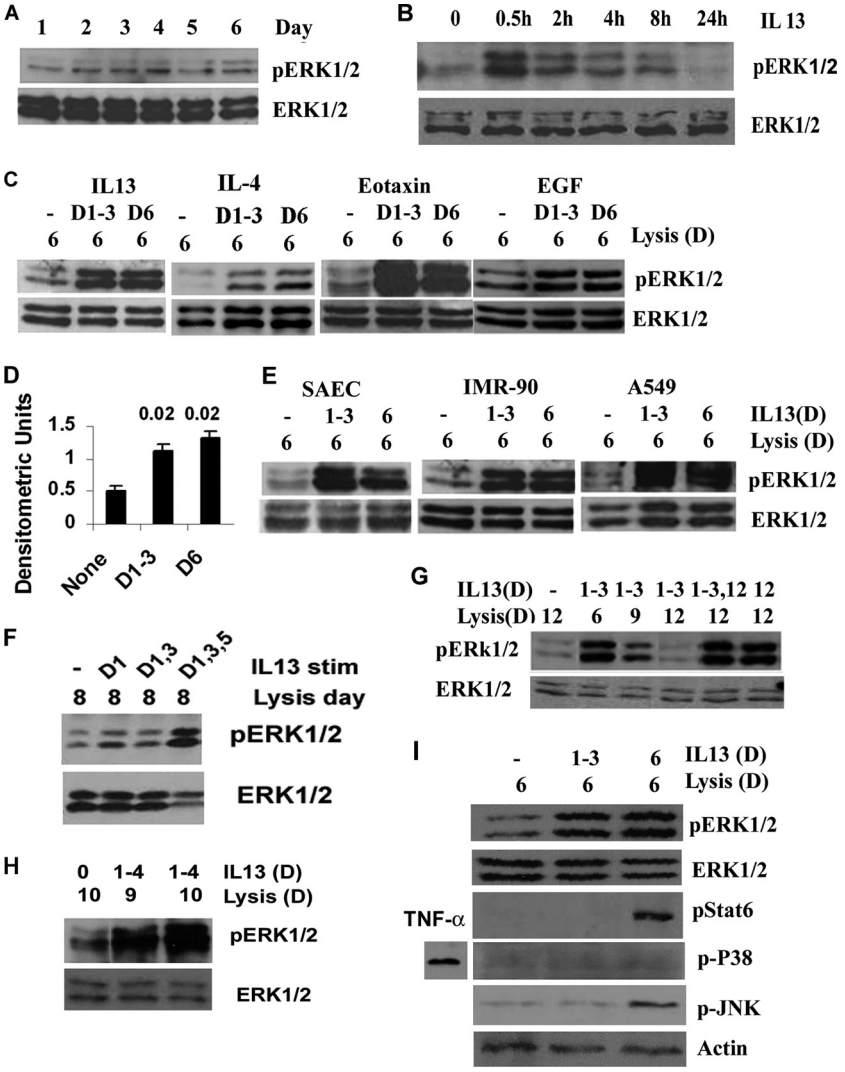

FIG. 1. Development of ERK1/2 bistability in human cells. (A) Basal phosphorylation of ERK1/2 in cultured airway epithelial cell line BEAS-2B studied over a period of 6 consecutive days without any stimulation. Following Western blotting with pERK1/2, the membrane was reprobed with an anti-ERK1/2 antibody ($n = 3$). (B) Kinetics of pERK1/2 in BEAS-2B cells stimulated with IL-13 (20 ng/ml), as measured by Western blotting ($n = 3$). (C) BEAS-2B cells were stimulated with IL-13 (10 ng/ml), IL-4 (10 ng/ml), eotaxin (10 ng/ml), or EGF (100 ng/ml) separately for 1 h daily for 3 consecutive days. The cells were washed 3 times after each stimulation and cultured without stimulation for 3 additional days after the last stimulation (samples labeled D1-3). One set of controls was stimulated and washed with buffer (−), and another set of controls was stimulated on day 6 with IL-13 or the other cytokines 1 h before lysis (D6). All these samples were lysed on day 6 and Western blotted for pERK1/2 ($n = 3$ to 6). (D) Densitometric analysis of pERK1/2 expression after repeated IL-13 stimulation as presented in panel C, top ($n = 6$). Statistical significance (P values) is shown above the bars. (E) Small airway primary epithelial cells (SAEC), the lung fibroblast cell line IMR-90, and the lung alveolar carcinoma cell line A549 were treated with IL-13 as described for panel D and Western blotted for pERK1/2 ($n = 3$). (F) BEAS-2B cells were stimulated with IL-13 on alternate days and then lysed on day 8 ($n = 3$). (G) BEAS-2B cells were stimulated with IL-13 for 3 consecutive days (days 1 to 3) and then lysed on the indicated days and Western blotted for pERK1/2. Selected stimulated or nonstimulated samples were also stimulated on day 12 before lysis ($n = 3$). (H) Effect of 4 days of stimulation. BEAS-2B cells were stimulated with buffer or IL-13 for 1 h daily for 4 consecutive days and Western blotted on the indicated lysis days ($n = 3$). (I) BEAS-2B cells were stimulated with IL-13 as described for panel C. The cell lysate was Western blotted using antibodies against pERK1/2, ERK1/2, pSTAT6, p-p38 MAPK, and pJNK. For p-p38, an aliquot of cells was additionally stimulated with TNF-α as a positive control. The pJNK membrane was reprobed with an anti-β-actin antibody to demonstrate protein loading ($n = 4$).

PP2 from day 4 to day 6 following IL-13 stimulation on days 1 to 3. PP2 treatment significantly inhibited ERK1/2 phosphorylation but partially inhibited Sprouty 2 expression (Fig. 3A). Next we studied the SYF cell line, which has a null mutation for the most prevalent Src family kinases in fibroblasts, Src, Yes, and Fyn. Unlike epithelial cells (see previous experiments) and control fibroblasts, SYF cells did not express Sprouty 2 under basal conditions (Fig. 3B). Both acute and repeated stimulation induced low-level Sprouty 2 expression in these cells. However, ERK1/2 phosphorylation was severely impaired under both experimental conditions. The results suggest that Src family kinases are important for ERK1/2 phosphorylation and, to a lesser extent, Sprouty 2 expression following IL-13 stimulation. A previous report indicates that

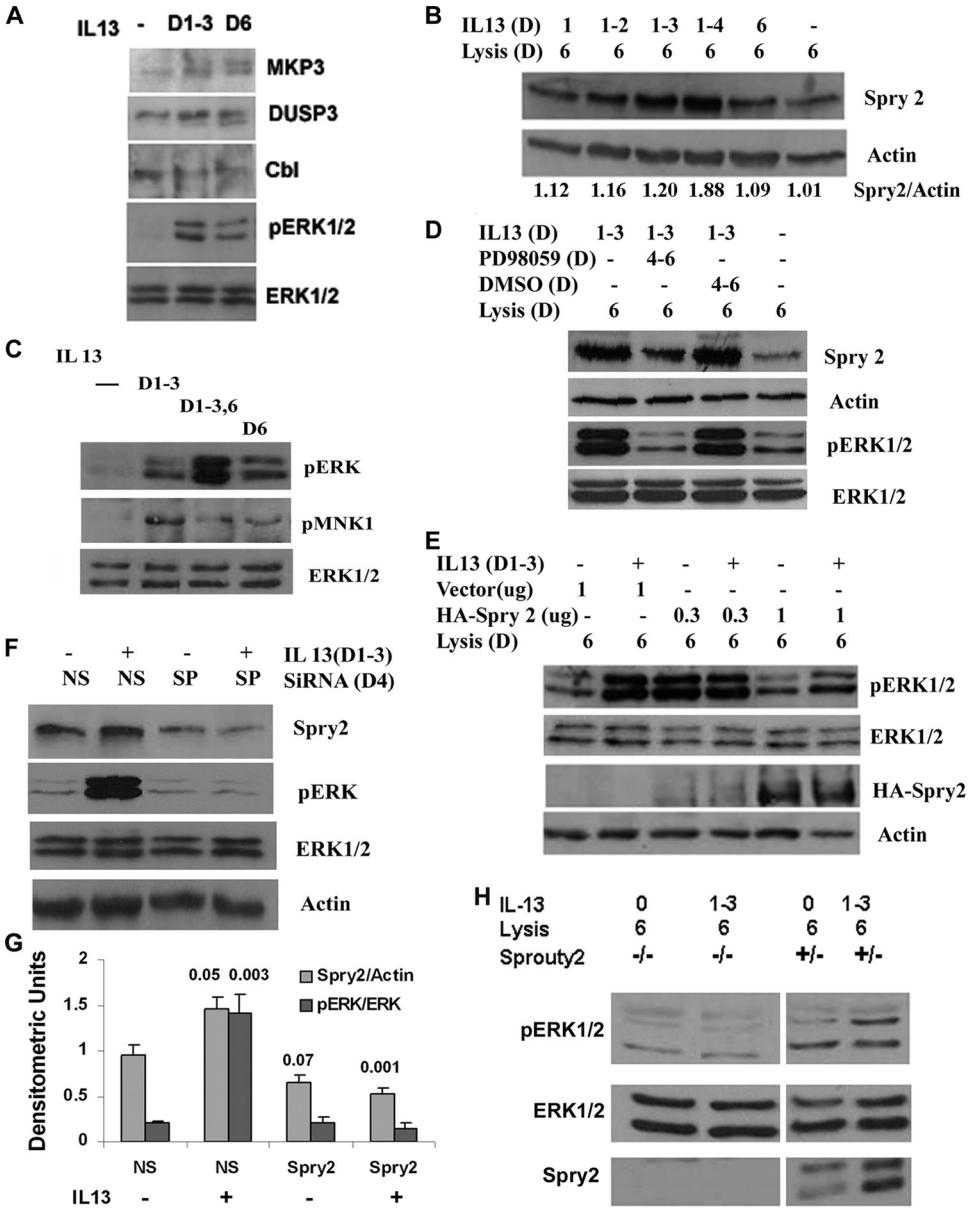

FIG. 2. Role of Sprouty 2 in sustained ERK1/2 activation. (A) Expression of dual-specific phosphatases MKP3 and DUSP3 and receptor-associated ubiquitin ligase Cbl in the repeated-stimulation model. BEAS-2B cells were stimulated repeatedly on days 1 to 3 or only once on day 6 and then Western blotted. The membranes were reprobed for ERK1/2 to demonstrate protein loading ($n = 3$). (B) Sprouty 2 expression after repeated stimulation. BEAS-2B cells were stimulated with IL-13 for the indicated number of days and then lysed and Western blotted on day 6. The membrane was reprobed for β-actin ($n = 4$). (C) Mnk1 phosphorylation. BEAS-2B epithelial cells were stimulated with IL-13 as described for Fig. 1C and then Western blotted for pERK1/2 and pMnk1. The membrane was reprobed with an anti-ERK1/2 antibody ($n = 3$). (D) Effect of a MEK inhibitor on Sprouty 2 expression. BEAS-2B cells were treated with IL-13 as described for Fig. 1C and then incubated with the MEK1/2 inhibitor PD98059 or the diluent DMSO on days 4 to 6. The cell lysate was Western blotted for Sprouty 2 and pERK1/2. The membranes were reprobed with anti-ERK1/2 and anti-β-actin antibodies, respectively ($n = 3$). (E) Effect of overexpression of Sprouty 2 on pERK1/2. BEAS-2B cells were transfected with two concentrations of a hemagglutinin (HA)-tagged Sprouty 2 expression vector or a control vector and then stimulated with IL-13 as described for Fig. 1C. The cell lysates were Western blotted with anti-pERK1/2 and anti-HA antibodies and reprobed for ERK1/2 and β-actin, respectively ($n = 3$). (F) Effect of Sprouty 2 knockdown on sustained pERK1/2. BEAS-2B cells were treated with siRNA for Sprouty 2 (SP) or luciferase (nonspecific [NS]) and then stimulated with IL-13 as described for Fig. 1C. The cell lysates were Western blotted for Sprouty 2 and pERK1/2. The membranes were reprobed for actin and ERK1/2, respectively ($n = 4$). (G) Densitometric analysis of Sprouty 2 and pERK1/2 expression as presented for panel F. Statistical significance (P value) compared to the NS and IL-13$^-$ sample is shown above the bars. (H) Effect of Sprouty 2 knockout on pERK1/2. Mouse embryonic fibroblasts with Sprouty 2 homozygous (−/−) and heterozygous (+/−) null deletions were stimulated with IL-13 as described for Fig. 1C. The cell lysates were Western blotted for pERK1/2 and Sprouty 2. The pERK1/2 membrane was reprobed for ERK1/2 ($n = 3$).

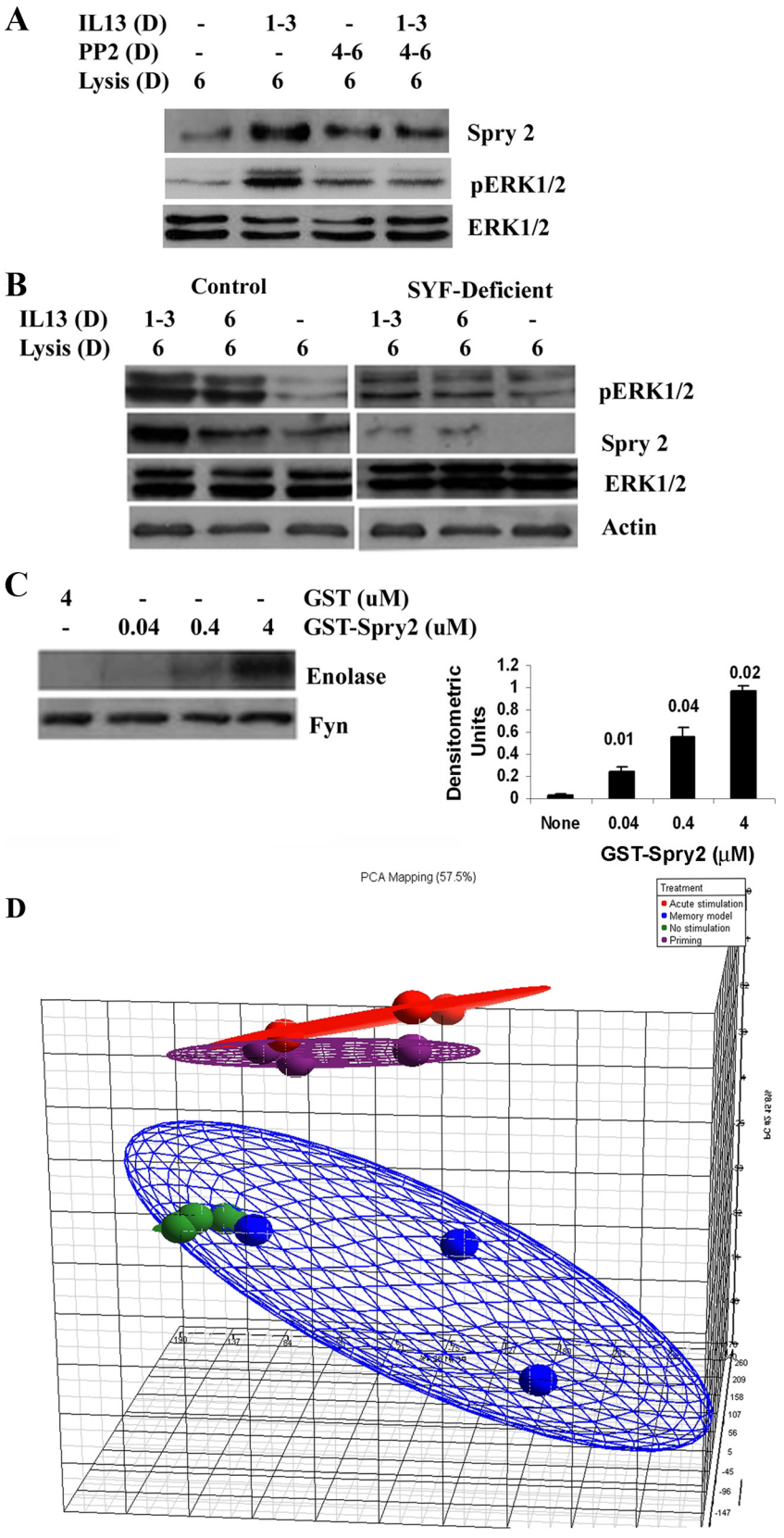

FIG. 3. Role of Src family kinases in sustained ERK1/2 activation and microarray data analyses. (A) Effect of Src family kinase inhibition. BEAS-2B cells were stimulated with IL-13 as described for Fig. 1C and then incubated with the Src family kinase inhibitor PP2 on days 4 to 6. The cell lysates were Western blotted for Sprouty 2 and pERK1/2 ($n = 3$). (B) Mouse embryonic fibroblasts with homozygous null mutation for Src,

TABLE 1. Statistical analyses of GeneChip microarray data for the 4 study groups

Compared groups	*P*	No. of significant *P* values
No stimulation vs acute stimulation	0.0030314	2,016
No stimulation vs repeated stimulation	0.000601468	40
No stimulation vs priming model	0.00196078	1,304
Repeated stimulation vs acute stimulation	0.00171418	1,140
Repeated stimulation vs priming	0.00140142	932
Priming vs acute stimulation	0.00013533	9

Sprouty 2 is a direct substrate for Src family kinases (26). However, the effect of Sprouty 2 on Src family kinases is unknown. Sprouty 2 has a proline-rich sequence with the SH3-binding motif PXXPXR (residues 301 to 309) (26). SH3-binding motifs can activate Src family kinases by disrupting the internal SH3 domain-linker region interaction (35). To determine whether Sprouty 2 could directly activate the Src family kinase Fyn, we performed an *in vitro* kinase assay using purified recombinant GST-Sprouty 2. Recombinant Sprouty 2 stimulated the enzymatic activity of Fyn, which induced enolase (substrate) phosphorylation *in vitro* (Fig. 3C).

Global gene expression profile in cells with sustained ERK1/2 phosphorylation. In order to assess the functional consequences of sustained ERK1/2 phosphorylation in our experimental model, we performed GeneChip analysis of the BEAS-2B cell mRNA expression profiles of four groups of cells: (i) control cells cultured for 6 days without IL-13 stimulation; (ii) cells stimulated with IL-13 (1 h/day) on days 1 to 3 and then rested for the next 3 days (repeated-stimulation or memory model); (iii) cells cultured for 6 days and then stimulated for 1 h before lysis on day 6 (acute stimulation); and (iv) cells stimulated on days 1 to 3, rested on days 4 and 5, and then restimulated on day 6 for 1 h before lysis ("priming" model). A single stimulation increased the expression of 2,016 transcripts (Table 1). To our surprise, cells from the repeated-stimulation model increased the expression of only 40 transcripts. Repeated stimulation actually downregulated the expression of many genes below the baseline level for nonstimulated cells. This is reflected by the reduced number of upregulated genes (a total of 1,304 transcripts) in the priming model. Despite the reduced total number of upregulated genes, we did observe a priming effect on many genes. Some of the relevant genes that were primed (induced at a level significantly higher than that for the acute model) include the CCL3, CLCA1 (calcium-activated chloride channel 1), EGF receptor (EGFR), FOS, RAB5B, MAP3K11, MAPK8IP1, and SPRY4 genes. Growth- and proliferation-related genes that were upregulated in the priming model are shown in Table 2. Principal component analysis of the expression profile showed a distinct pattern of activation state (Fig. 3D) in these four cell populations. We recognize that one sample from the repeated-stimulation model (memory model) clustered with the nonstimulated cells, which is likely to reflect a lack of stimulation due to an experimental error.

Some of the genes that were upregulated specifically in the repeated-stimulation model (i.e., not induced in the acute model) and that are relevant to the MAPK pathway and epithelial function include (alphabetical order) the ARRB1 (beta 1 arrestin), CCL8 (MCP2), CCL26 (eotaxin 3), CCL27, CDC42 eff 2, IL17RD (Sef), MAP2K2 (MEK2), MAP3K10 (MLK2/MST), MAP3K11 (MLK3), MAP4K1 (HPK1, Ste20-like kinase), MAPK8IP1 (JIP1), MKNK1 (Mnk1), MUC5B, PFKFB4, RAB4B, and UNC119 genes (Table 2). Of these genes, the ARRB1, CDC42 eff 2, IL17RD, MAP2K2, MAP3K10, MAP3K11, MAP4K1, MAPK8IP1, and MKNK1 genes are known to function upstream or downstream of ERK1/2 and regulate ERK1/2 activity. We have already shown increased phosphorylation of Mnk1 in our model. Sprouty 2 mRNA was not upregulated in the microarray screen from the memory model but was increased in the acute and priming models. We speculate that the increased protein level after repeated stimulation results from Mnk1-mediated phosphorylation of Sprouty 2 and inhibition of its degradation. Increased expression of UNC119 mRNA is of interest. Unc119 is an activator of Src family kinases including Fyn, which signals through the ERK1/2 pathway (14).

MAPK signaling-related genes that were downregulated in the repeated-stimulation model compared to nonstimulated control cells include the BIM, CBL, DUSP4 (MKP2), and IL13RA1 genes. BIM is a proapoptotic molecule, whose level and activity are primarily regulated at the protein level. Nonetheless, a reduced level of BIM mRNA could contribute to epithelial cell survival. We confirmed the reduced expression of Cbl at the protein level in the repeated-stimulation model (Fig. 2A). The reduced level Cbl could also contribute to increased Sprouty 2. DUSP4 (MKP2) is a MAPK-specific nuclear phosphatase, which has been shown to mediate stress-induced cellular apoptosis (50). Reduced nuclear DUSP4 delays cell senescence (48).

Reduced nuclear translocation and increased endosomal localization of pERK1/2 in the repeated-stimulation model. In order to examine the apparent discrepancy between increased ERK1/2 phosphorylation and reduced gene transcription, we performed immunofluorescent staining (IFS) of cells for pERK1/2. IFS showed substantial nuclear translocation of

Yes, and Fyn (SYF) and control fibroblasts were treated with IL-13 as described for Fig. 1C and then Western blotted for pERK1/2 and Sprouty 2 ($n = 4$). (C) Effect of recombinant Sprouty 2 on Fyn kinase activation. (Left) Sprouty 2 was expressed as a GST-Sprouty 2 fusion protein, and the purified GST and GST-Sprouty 2 (Spry 2) were used in a Fyn immune complex kinase assay in the presence of [γ-^{32}P]ATP and enolase as a substrate. (Right) Densitometric analysis of phosphorylated enolase bands (from the left panel) from 4 separate experiments. Statistical significance (*P* values) compared to "none" is shown above the bars. (D) Principal component analysis of the GeneChip data. No stimulation, control cells incubated with buffer instead of IL-13 (green); memory model, cells repeatedly stimulated with IL-13 on days 1 to 3 (blue); acute stimulation, cells stimulated with IL-13 for 30 min on day 6 (red); priming, cells repeatedly stimulated with IL-13 on days 1 to 3 and then restimulated on day 6 (purple).

TABLE 2. Selected genes whose expression was altered in the repeated-stimulation and priming models

Gene	Description or alternate designation	Function(s) of protein
Genes upregulated in the repeated-stimulation model		
ARRB1	Arrestin beta 1 gene	Scaffold, activates ERK1/2
CDC42 eff 5		
CCL8	*MCP2*	
CCL26	Eotaxin 3 gene	
CCL27	*CTACK*	
IL17RD	*Sef*	Receptor for IL-17D; also functions as an ERK1/2 scaffold in the Golgi apparatus
MAP3K10	Mixed-lineage kinase 2 (MLK2) gene	
MAP3K11	Mixed-lineage kinase 3 (MLK3) gene	
MAP4K1	*HPK1*	
MAPK8IP1	JNK-interacting protein 1 (JIP1) gene	
MAP2K2	MAP ERK kinase 2 (MEK2) gene	Activates ERK1/2
MKNK1	*Mnk1*	Cap-dependent protein translation
MUC5	Mucin gene	
PFKFB4	6-Phosphofructo-2-kinase/fructose-2,6-biphosphatase 4 gene	Aerobic glycolysis, cell proliferation
RAB4B	*Rab4b*	Early endosome-associated GTPase
SPRY4	Sprouty 4 gene	Development/regulation of signaling
UNC119	*HRG4*	Activates Src kinases
Genes downregulated in the repeated-stimulation model		
BIM		Proapoptotic molecule
CBL	*Cbl*	Receptor-associated ubiquitin ligase, degrades Sprouty
DUSP4	Dual-specific phosphatase gene	Dephosphorylates nuclear ERK1/2
IL13RA1	IL-13 receptor alpha 1 gene	
PFKFB2	6-Phosphofructo-2-kinase/fructose-2,6-biphosphatase 2 gene	Aerobic glycolysis, cell proliferation
Genes upregulated in the priming model		
CDYL	Chromodomain protein Y-like gene	Chromatin assembly/disassembly
CHMP4A	Chromatin-modifying protein 4A gene	
CLCA1		Calcium-activated chloride channel regulating mucus
EGFR	EGF receptor gene	
EGR1	Early growth response 1 gene	Regulation of transcription
EMP3	Epithelial membrane protein 3 gene	Negative regulation of proliferation
ETV5	*ets* variant gene 5	Regulation of transcription
FOS		Transcription
GPATCH1	Gpatch domain containing 1 gene	Intracellular; nucleic acid binding
JAG1	*jagged 1*	Cell fate determination/morphogenesis of epithelial sheet
JMJD6	Jumonji domain containing 6 gene	Development/differentiation
PLK3	polo-like kinase 3 gene	Regulation of cell cycle
RAB5B		Early endosome-associated GTPase
SERTAD1	serta domain containing 1 gene	Regulation of cyclin protein kinase
ZNF264		Regulation of transcription

pERK1/2 upon acute (D6) stimulation of cells with IL-13 (Fig. 4A). In contrast, repeated stimulation (days 1 to 3) caused only modest translocation of pERK1/2 to the nucleus. The cytosolic pERK1/2 in the repeated-stimulation model could be redirected to the nucleus upon a priming stimulation (days 1 to 3 and 6). The results suggest that pERK1/2 is segregated in the cytosolic compartment in the repeated-stimulation model and that the cells in this model are primed for heightened nuclear activity of pERK1/2. The cytosolic sequestration of ERK1/2 has previously been observed under specific experimental conditions (12).

Next we examined the enzymatic activity of pERK and its functional consequences in the repeated-stimulation model. An *in vitro* kinase assay using myelin basic protein as a substrate showed significant enzymatic activity of pERK1/2 (Fig. 4B). To examine the transcriptional consequences of pERK1/2, we studied the expression of c-Fos, c-Jun, JunB, and JunD. pERK1/2 in the acute-stimulation model induced the expression of c-Fos and JunB. In contrast, a similar level of pERK1/2 in the repeated-stimulation model induced only a modest level of c-Fos and no JunB. Levels of induction of c-Jun were comparable among the acute-, repeated-, and priming stimulation models. Levels of JunD expression were similar in all study samples. The differential expression of the AP1 transcription factors provides

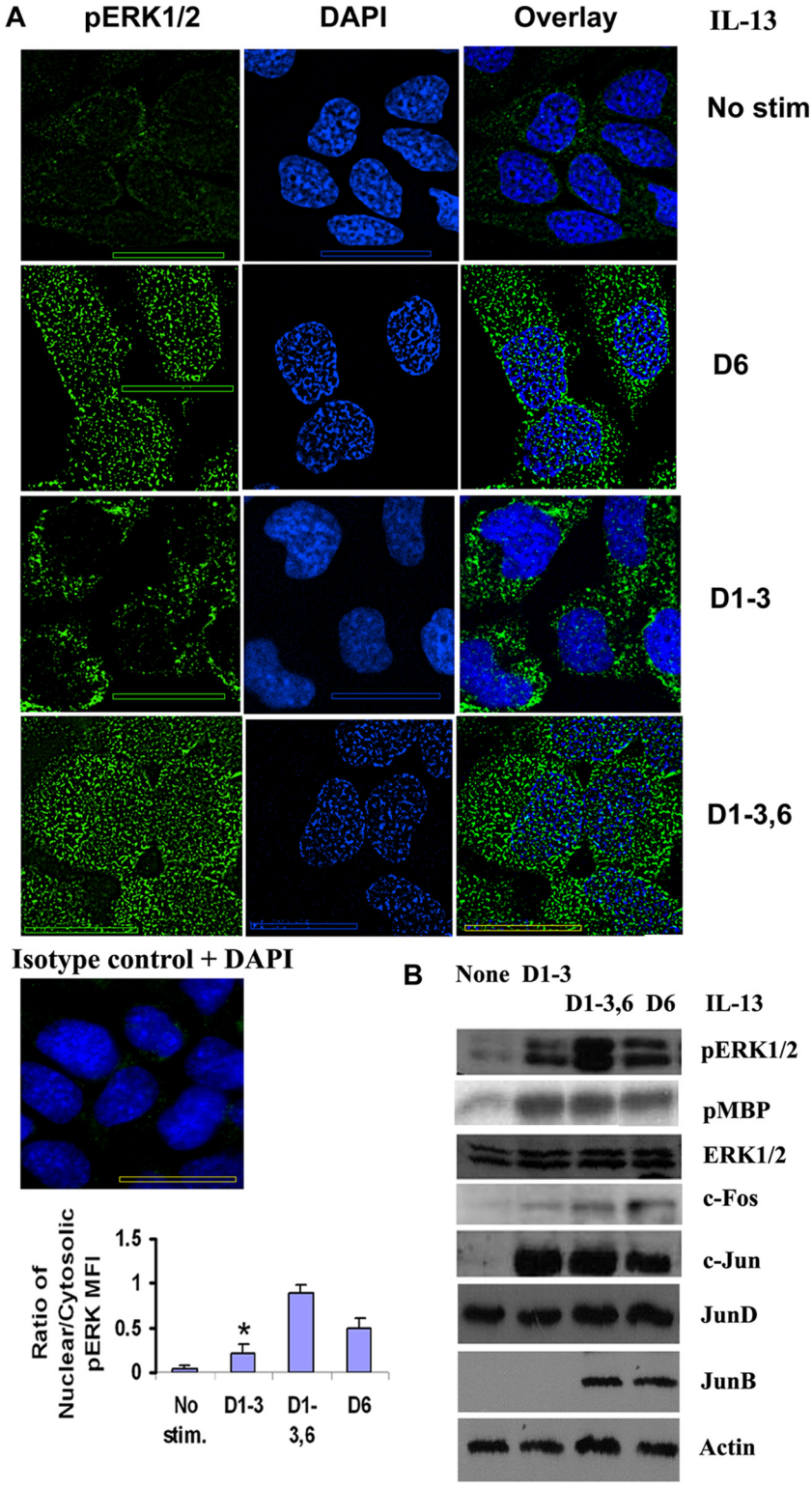

FIG. 4. Nuclear translocation of pERK1/2. (A, top) BEAS-2B cells were left unstimulated (no stim), stimulated with IL-13 once on day 6 (D6), or stimulated (1 h per day and then washed) repeatedly on days 1 to 3 and then either rested on days 4 to 6 (D1-3) or stimulated again on day 6 (D1-3,6). The cells were then fixed on day 6 and processed for immunofluorescent staining using a mouse anti-pERK1/2 antibody and counterstained with DAPI (4′,6-diamidino-2-phenylindole). Z-stack images (magnification, ×100) were captured and deconvolved with no neighbors using the software Metamorph, v.7. $n = 7$; scale bar = 10 μm. (Middle) Immunostaining of epithelial cells with a mouse IgG1 isotype antibody (control for the anti-pERK1/2 antibody). The slide was counterstained with DAPI ($n = 3$). (Bottom) Quantification of the mean fluorescence intensity (MFI) of nuclear and cytosolic pERK1/2 by the software Metamorph, v.7.0. *, $P < 0.04$ compared to D6 and D1-3,6. $n = 7$. (B) Kinase activity of pERK1/2 and its effect on AP1 complex proteins. BEAS-2B cells were stimulated with IL-13 as described for panel A. Cells were lysed, and one sample was used in an immune complex kinase assay for ERK1/2 using myelin basic protein (MBP) as a substrate. The incorporation of [γ-^{32}P]ATP into MBP was detected by autoradiography. The membrane was reprobed for ERK1/2 ($n = 4$). Other samples were Western blotted for pERK1/2, c-Fos, c-Jun, JunB, and JunD. The c-Fos membrane was reprobed for actin ($n = 3$).

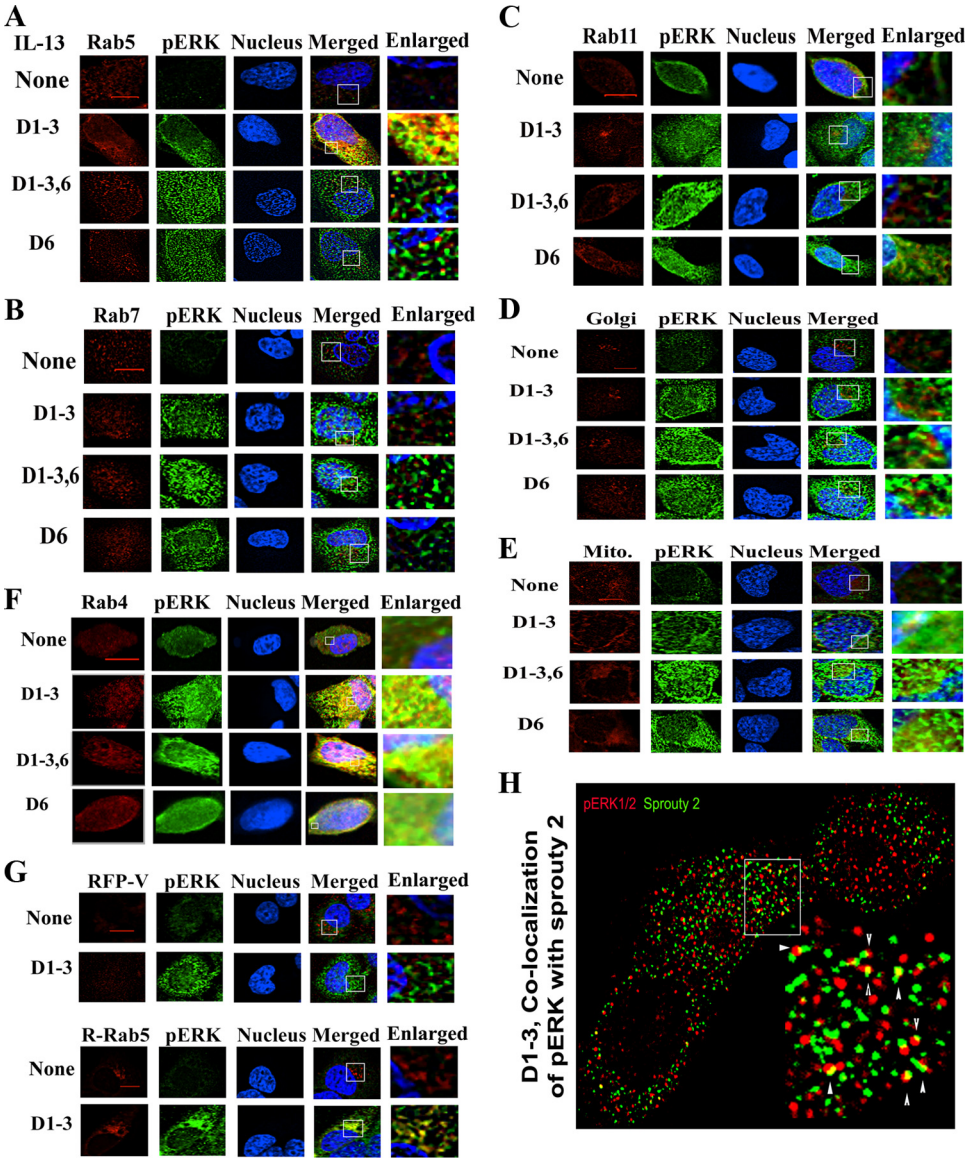

FIG. 5. Endosomal localization of pERK1/2. BEAS-2B cells were stimulated as described for Fig. 4A and then processed for double-immunofluorescent staining for pERK1/2 (green) and the early, late, and recycling endosomal markers Rab5 (A), Rab7 (B), and Rab11 (C) (red), respectively, on day 6. The nucleus was stained blue with DAPI ($n = 4$). Z-series images (magnification, ×100) were deconvolved with no neighbors using the software Metamorph, v.7, and presented as maximal projection ($n = 4$). Scale bars = 5 μm. The right panels represent higher magnifications of the boxed areas. (D and E) Immunostaining with Golgi (GM130) (D) and mitochondrial (Mitotracker) (E) markers ($n = 4$). (F) Colocalization of pERK1/2 with Rab4 ($n = 4$). (G) Colocalization with red fluorescent protein (RFP)-Rab5. BEAS-2B cells were stimulated with IL-13 as described for Fig. 4A and then transfected with the red fluorescent protein control vector (RFP-V) or RFP-Rab5 fusion construct (R-Rab5) on day 4. The cells were stained for pERK1/2 on day 6 and counterstained with DAPI. Z-series images were deconvolved, and selected images are presented ($n = 3$). (H) Colocalization of Sprouty 2 with pERK1/2. BEAS-2B cells were stimulated as described for Fig. 4A and then double stained for pERK1/2 (green) and Sprouty 2 (red). Z-series images (magnification, ×100) were 3-dimensionally deconvolved with the point spread function and Metamorph software. The boxed area is enlarged in the bottom right frame. Colocalization (yellow) is shown with arrowheads.

an explanation for the microarray data in our experimental models.

Next we examined the cytosolic localization of pERK1/2 in the repeated-stimulation model by double immunofluorescent staining using specific markers for various endosomes, the Golgi apparatus, and mitochondria. We observed significant colocalization of pERK1/2 with $Rab5^+$ early endosomes but not with $Rab7^+$ late endosomes or $Rab11^+$ recycling endosomes (Fig. 5A to C and 6A). There was low-level colocalization of pERK1/2 with Rab5 in the acute-stimulation model. The Golgi apparatus and mitochondria did not colocalize with pERK1/2 (Fig. 5D and E). The endosomal distribution of Rab5 partially overlaps with that of Rab4. In accordance, we observed colocalization of Rab4 with pERK1/2 (Fig. 5F) in the repeated-stimulation and priming models. There was also a low-level colocalization with pERK1/2 after acute stimulation.

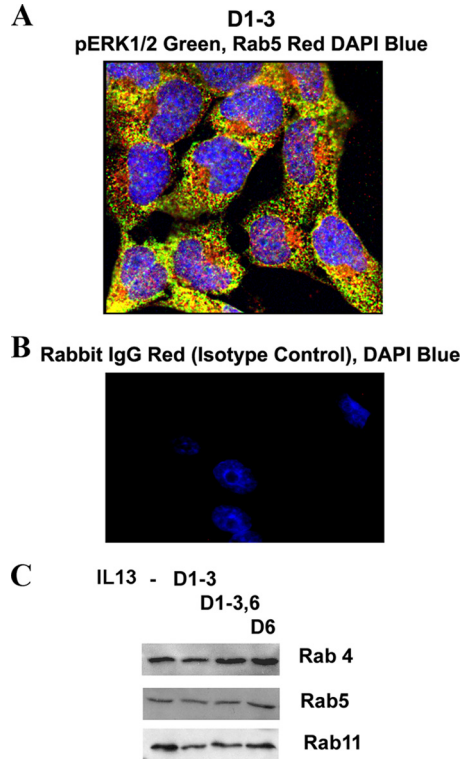

FIG. 6. Subcellular localization of pERK1/2. (A) Colocalization of pERK1/2 with Rab5. An overlay picture of pERK1/2 (green) and Rab5 (red) showing colocalization (yellow) in multiple cells is shown ($n = 6$). (B) Immunostaining with a rabbit IgG antibody (control for antibodies against Rab4, Rab5, Rab7, Rab11, GM130, and Sprouty 2) and counterstaining with DAPI ($n = 3$). (C) Expression of Rab4, Rab5, and Rab11 in epithelial cells. BEAS-2B cells were stimulated with IL-13 as described for Fig. 4A and then Western blotted for Rab4, Rab5, and Rab11 ($n = 3$).

In order to confirm the colocalization using another approach, we transfected cells with Rab5-green fluorescent protein (GFP) and then subjected them to repeated IL-13 stimulation. We observed colocalization of Rab5-GFP with pERK1/2 (Fig. 5G). The protein levels of Rab5 and Rab11 were largely unchanged under the stimulation protocols (Fig. 6C). However, Rab4 was induced in the acute-stimulation model. Cytokine regulation of Rab expression has recently been reported (2). Collectively, the results suggest that pERK1/2 is largely segregated in the $Rab5^+$ and $Rab4^+$ endosomal compartments.

Sprouty 2 has previously been shown to transiently colocalize with $Rab5^+$ endosomes upon stimulation (16). Since Sprouty 2 is important for sustained ERK1/2 phosphorylation, we asked if the former colocalized with pERK1/2 in the repeated-stimulation model. We observed a low-level colocalization of Sprouty 2 with pERK1/2 in the repeated-stimulation model (Fig. 5H).

Functional consequences of bistable pERK1/2. (i) Effect on cell proliferation. To define whether the self-sustained pERK1/2 is associated with increased cell proliferation, we performed a [^{3}H]thymidine incorporation assay of cells on days 4, 7, and 10 after repeated stimulation. There was no difference in thymidine uptake between the control cells and cells with sustained pERK1/2 (Fig. 7A). This is not a surprise given the reduced transcriptional activity in the repeated-stimulation model.

(ii) Effect on cell survival. We asked if sustained ERK1/2 activation provided any survival advantage to the cells. Epithelial cells are normally cultured in a growth factor-enriched medium. To study the effect on survival, we stopped adding the growth factor supplement to the basic culture medium after the induction of sustained pERK1/2. Growth factor withdrawal led to decreased survival of control cells over time (Fig. 7B), which was primarily due to apoptosis (Fig. 7C). Cells from the repeated-stimulation model survived longer after growth factor withdrawal than cells that were stimulated with IL-13 once or not stimulated at all. We examined selected survival- and apoptosis-promoting genes (Fig. 7D). BID was induced after single and repeated stimulation, although the effect of repeated stimulation on BID was modest. The expression of mRNA for BIM was reduced in the repeated-stimulation model, which confirms the microarray data. Further, the expression of mRNA for Bax, and especially for FOXO3a, was reduced in the repeated-stimulation model. The reduced expression of mRNA for the proapoptotic genes could provide a survival benefit. The expression of Bcl2 mRNA was largely unchanged in both models.

(iii) Priming effect on selected cytokine production. We asked if epithelial cells with sustained pERK1/2 were primed for increased function. For this purpose we focused on epithelial cell-secreted products that modulate the function of other cells. We studied the expression of the eotaxin 3 (CCL26), RANTES (CCL5), CCL20, stem cell factor, thymic stromal lymphopoietin (TSLP), interleukin-13, and matrix metalloproteinase 9 (MMP9) genes. Acute stimulation on day 6 induced the expression of mRNA for eotaxin 3, RANTES, MMP9, and CCL20 (Fig. 7E). Stimulation of cells with sustained pERK1/2 on day 6 induced a higher level of mRNA expression for eotaxin 3, RANTES, stem cell factor, and TSLP. This priming effect was absent for IL-13. The expression of MMP9 and CCL20 was actually downregulated.

Role of Rab5 in sustaining endosomal pERK1/2 and prolongation of cell survival. Since pERK1/2 is compartmentalized to $Rab4^+$ and $Rab5^+$ endosomes in our experimental model, we asked if they were important for maintaining ERK1/2 phosphorylation and prolonged cell survival. To determine this, we knocked down the expression of Rab4 and Rab5 using siRNA and examined the persistence of pERK1/2. Rab5-deficient but not Rab4-deficient cells were unable to sustain pERK1/2 in the repeated-stimulation model (Fig. 8A and B). The loss of Rab5 led to reduced cell survival in the repeated-stimulation model (Fig. 8C).

Repeated EGF stimulation induces neurite growth in PC12 cells. In a well-known experimental paradigm of the neuron-like pheochromocytoma cell line PC12, NGF and EGF induce transient and sustained ERK1/2 activation, respectively (38, 47). Transient ERK1/2 activation by EGF promotes cell proliferation, whereas sustained activation by NGF induces differentiation and neurite outgrowth. Since repeated EGF stimulation induced sustained ERK1/2 activation in our model, we asked if this would induce neurite outgrowth in PC12 cells. To determine this, we treated PC12 cells with EGF 1 h a day for 1, 2, and 3 consecutive days. Neurite growth was studied on day 5 and compared with that after treatment with NGF. We ob-

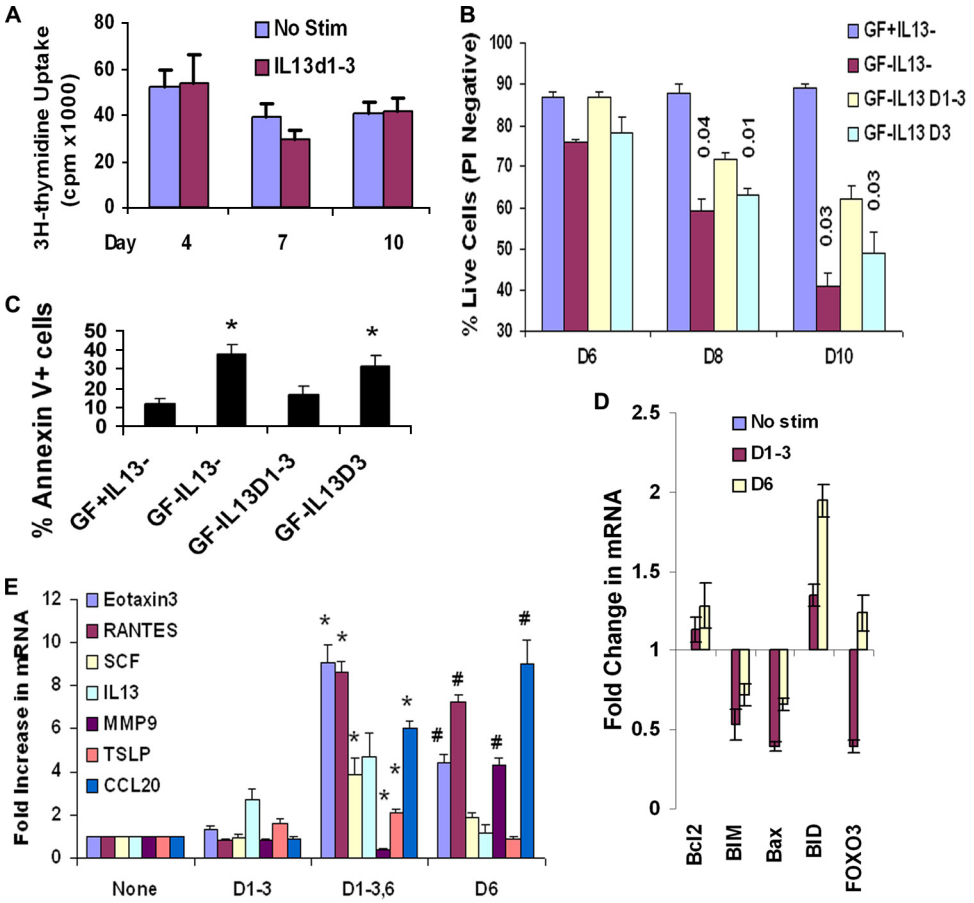

FIG. 7. Biological relevance of sustained ERK1/2 activation. (A) Effect on proliferation. BEAS-2B cells were stimulated with IL-13 as described for Fig. 4A and then cultured in the presence of [^{3}H]thymidine overnight before the conclusion of the culture at the indicated time point. No Stim, no stimulation ($n = 3$). (B) Effect on cell survival. BEAS-2B cells were stimulated repeatedly with IL-13 (1 h per day) on days 1 to 3 (IL-13 D1-3) or only day 3 (IL-13 D3) and then cultured in basal medium with (GF+) or without (GF−) growth factor-enriched supplement. Cell survival was monitored on days 6, 8, and 10 by staining with propidium iodide (PI). Statistical significance levels compared to the day 1 to 3 samples are shown above the bars ($n = 4$). (C) Effect on apoptosis. BEAS-2B cells were stimulated with IL-13 as described for Fig. 4A, and cell apoptosis was measured on day 8 by flow cytometry following staining with annexin V and propidium iodide. *, $P < 0.04$ ($n = 3$). (D) Real-time PCR for mRNA for selected apoptosis-regulating genes. Fold changes in mRNA compared to that in nonstimulated cells are shown ($n = 3$). β-Actin and GAPDH (glyceraldehyde-3-phosphate dehydrogenase) genes were used as housekeeping gene controls. (E) Effect on cytokine/protease production. Real-time PCR results for eotaxin 3, RANTES, stem cell factor (SCF), IL-13, MMP9, TSLP, and CCL20 are shown. β-Actin and GAPDH genes were used as housekeeping gene controls. Fold increases in gene expression over that in nonstimulated cells are shown ($n = 6$). *, $P < 0.04$; #, $P < 0.02$.

served significant neurite outgrowth after repeated EGF stimulation, especially after 3 days of stimulation (Fig. 9). The degree of neurite outgrowth was lower with EGF than with NGF, indicating some inherent signaling differences between the receptors for these two ligands. Nonetheless, the induction of significant neurite outgrowth validates the basic principle of our repeated-stimulation approach in this well-characterized experimental model.

Endosomal pERK1/2 in the airway epithelium from a mouse model of chronic asthma. We were interested to find out if the bistable pERK1/2 staining pattern was present *in vivo* in the tissue from a patient with a chronic disease such as asthma. We chose allergic asthma because this disease is characterized by repeated exposure to environmental agents such as allergens. We investigated the pERK1/2 staining pattern in a mouse model of chronic asthma where we repeatedly exposed mice to three different allergens, dust mites, ragweed, and *Aspergillus* (DRA), 2 days a week for 8 weeks and then rested them for 3 weeks. We reported the persistence in this model of peribronchial inflammation, airway remodeling with epithelial hypertrophy, and airway hyperreactivity, which lasted longer than 3 weeks after the last allergen exposure (13). Immunofluorescence studies of the airway tissue from this model demonstrated significant pERK1/2 staining of airway epithelium and inflammatory cells (Fig. 10A). pERK1/2 immunostaining was predominantly localized to the cytosol and only minimally to the nucleus. Double-immunostaining studies with three-dimensional (3D) deconvolution showed a significant colocalization of pERK1/2 with Rab5$^+$ endosomes (Fig. 10B). The increased pERK1/2 immunostaining was confirmed by Western blotting for pERK1/2 and by kinase assay of the lung lysate (Fig. 10C). This was associated with an elevated expression of Sprouty 2 in the lung tissue from the asthma model (Fig. 10C).

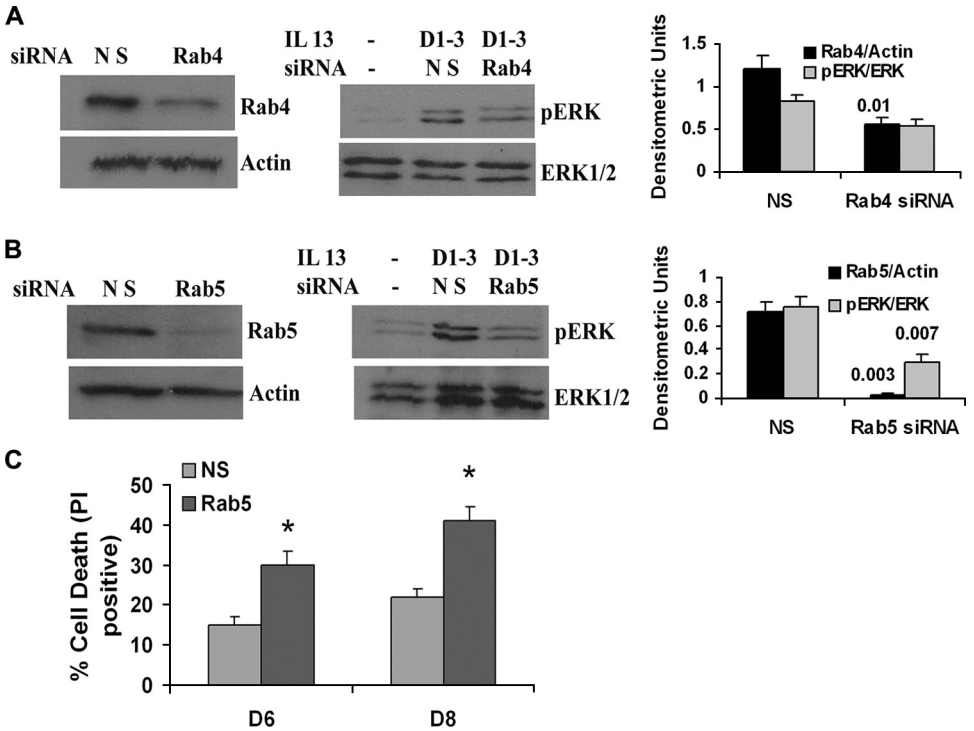

FIG. 8. (A and B) Effect of Rab4 and Rab5 knockdown on pERK1/2 and cell survival. BEAS-2B cells were stimulated with IL-13 on days 1 to 3 or left untreated and then transfected with Rab4a or Rab5a siRNA on day 4. A nontargeting siRNA that was directed against luciferase was used as a control (NS). Forty-eight hours later cells were divided into two aliquots; one aliquot was Western blotted for Rab4 (A, left), Rab5 (B, left), and pERK (A and B, middle) expression. Bar graphs at the right show densitometric analysis of the corresponding Western blot bands from 3 experiments. Statistical significance (*P* values) is shown above the bars. (C) One set of cells from the Rab5 knockdown experiment was further cultured for the indicated periods of time in the basic culture medium without the growth factor-rich supplement. At the conclusion the cells were stained with propidium iodide (PI) to determine cell survival. $n = 3$; $*$, $P < 0.04$.

Endosomal pERK1/2 in the airway epithelium from human asthma. Next we examined airway biopsy samples from asthmatic patients. We previously reported increased expression of pERK1/2 and Sprouty 2 in airway biopsy samples from asthmatic patients (30). There was a significant correlation between the expression level of pERK1/2 and asthma severity. We wondered if the pERK1/2 staining pattern has any resemblance with that in the bistable model. Epithelial cells from the biopsy samples demonstrated pERK1/2 immunostaining that was primarily localized to the cytosol, with modest nuclear staining (Fig. 10D and E). Further, double immunostaining followed by 3D deconvolution colocalized pERK1/2 with $Rab5^+$ endosomes in these biopsy samples (Fig. 10F).

DISCUSSION

Bistability of signaling molecules, especially that of the MAPK pathway, has been a subject of interest for a number of years. Xiong and Ferrell showed for the first time that ERK1/2 achieves a bistable form in frog oocytes following a single stimulation with progesterone (53). Bistability arises from a positive-feedback loop or a mutually inhibitory, double-negative-feedback loop. The authors have mathematically shown that when the strength of positive feedback exceeds a certain threshold the system shows hysteresis and becomes bistable. Since then numerous studies that addressed the theoretical basis for and experimental approaches to establishing bistability have been published. Bashor et al. have shown that engineered recruitment of the positive-feedback adapter Ste50 to the mating MAPK scaffold Ste5 changed the steady-state output of the MAPK pathways in *Saccharomyces cerevisiae* and led to a more switch-like digital output (1). While the theoretical basis for bistability in ERK1/2 and its upstream molecules such as Sos and Ras is quite strong, most previous studies relied on nonphysiological approaches to demonstrate ERK1/2 bistability. Frequently, this involved targeted overexpression of certain upstream molecules. In this paper we demonstrate for the first time that ERK1/2 achieves a bistable form, and manifests a digital output in normal human cells following repeated exposure to physiologically relevant stimuli. This bistability is accomplished through the induction of an intracellular positive-feedback loop.

Sprouty 2 is an adapter molecule that has been shown to up- or downregulate ERK1/2 activation depending upon the cell type and stimulating agent. Sprouty 2 binds to Grb2, FRS2, Shp2, Gap1, Raf, FGFR2b, and Sos1 (17, 44); Cbl (9); caveolin 1 (19); Hrs (23); Tesk 1 (4); PTP1B (54); PTEN (8); and SIAH-2 (36). Sprouty 2 inhibits FGF-stimulated ERK1/2 signaling by interacting with Grb2 (17). Conversely, it augments EGF-stimulated ERK1/2 signaling by interacting with Cbl (9) and Tesk 1 (4). Sprouty 2 functioned as a positive regulator of sustained ERK1/2 phosphorylation in our model. Cells with a genetically null mutation as well as Sprouty 2 knockdown were

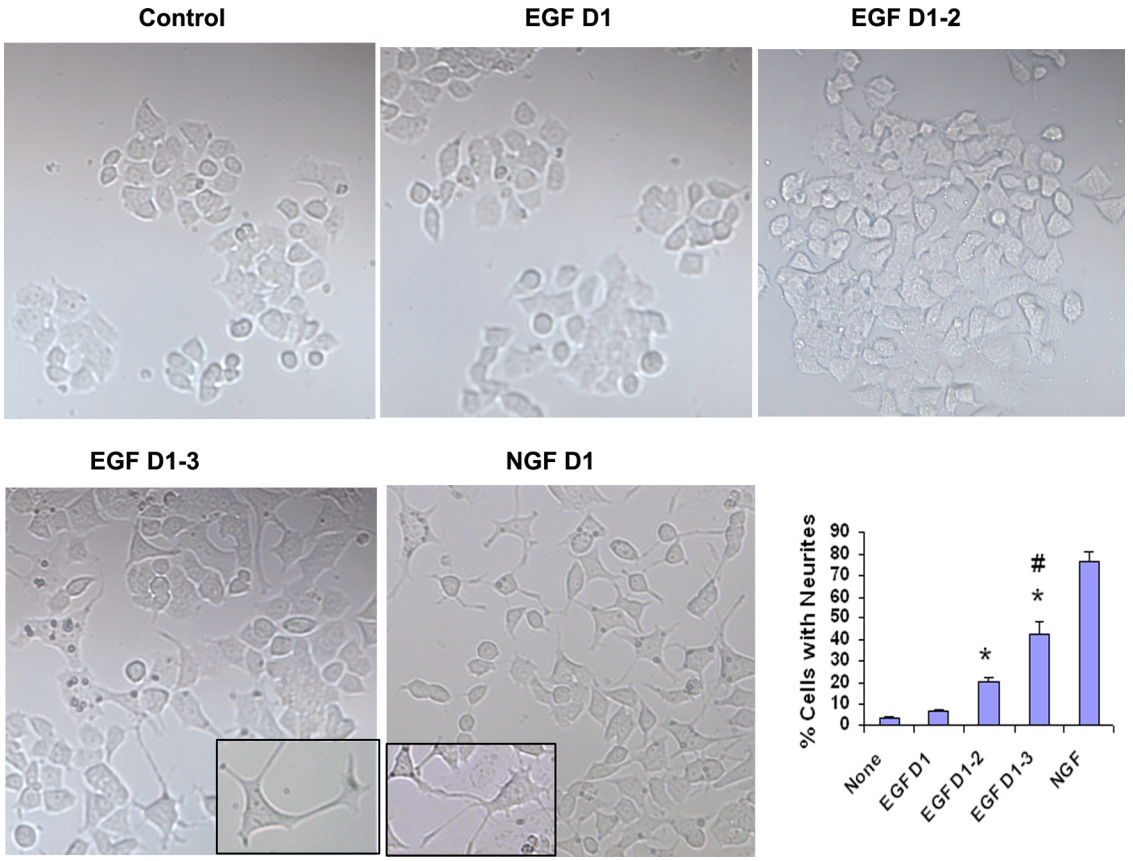

FIG. 9. Neurite growth in PC12 cells. PC12 cells were stimulated once with NGF on day 1 or with increasing frequency with EGF (day 1, days 1 and 2, and days 1 to 3). Images of neurite outgrowth were captured on day 5 using a 10× objective. Neurite outgrowth of 200 cells per culture and from four different cultures was counted for statistical analyses. *, $P < 0.01$ compared to no stimulation (none); #, $P = 0.01$ compared to NGF ($n = 4$).

unable to sustain ERK1/2 phosphorylation. Repeated stimulation of cells led to sustained Sprouty 2 induction that was associated with a simultaneous increase in phospho-Mnk1, a kinase known to phosphorylate and stabilize Sprouty 2 (6). It should be noted that the positive regulation of ERK1/2 activation occurs only when the Sprouty 2 level is increased at a moderate level. A high level of overexpression of Sprouty 2 actually inhibits ERK1/2 phosphorylation, which is consistent with the dual mode of action of this adapter molecule. We have uncovered a novel mechanism which involves a direct activation of Fyn kinase by Sprouty 2. We believe that moderately increased expression of Sprouty 2 leads to preferential activation of Fyn kinase in the endosomal compartment, followed by sustained ERK1/2 activation. A high level of overexpression is likely to cause a differential interaction with other signaling proteins, e.g., Grb2, which leads to ERK1/2 inhibition.

Bistability of ERK1/2 has previously been shown to arise from the membrane-associated nanoclusters of various Ras isoforms (45). In our model the bistable ERK1/2 was localized to a specific endosomal compartment. Endomembranes are derived from cell membranes. It is possible that appropriate nanoclusters of Ras are present on endomembranes and that these nanoclusters generates a digital output of ERK1/2 in our model. Previously, Sprouty 2 was shown to localize to $EEA1^+$ and $Rab5^+$ early endosomes (23). Sprouty 2 competes with Tsg101 for binding to Hrs, a multidomain protein belonging to the ESCORT family of proteins. This leads to slower degradation of the EGF receptor. We have not examined the role of Hrs and Tsg101 in our experimental model yet.

Sustained ERK1/2 activation in the $Rab5^+$ endosomal compartment led to increased cell survival. Rab5 knockdown caused increased cell death, which points to a novel role of Rab5 in promoting cell survival. In this context it is interesting to note that Rab7 promotes apoptosis following growth factor withdrawal (40). Survival-promoting activity has been ascribed to a number of Rab5-associated molecules including Appl1 and -2 (adaptor protein containing *P*H domain, *P*TB domain, and *l*eucine zipper motif) (37, 43) and Alsin (21, 46). Appl1 and -2 are essential for cell survival during development (43), and they interact with FOXO1a, major regulator of the cell cycle and cell survival (37). Rab5 interacts with the myosin complex (49). Dynein light chains, a component of the myosin complex, sequester a number of proapoptotic molecules such as BIM and BMF (7) and protect cells from apoptosis. It is possible that Rab5 promotes survival indirectly by sequestering BIM and BMF. Thus, there are a number of pathways by which Rab5 and Rab5-associated ERK1/2 could promote cell survival.

We have previously shown that pERK expression in the airway epithelium positively correlates with the severity of asthma (30). One of the determinants of asthma severity is

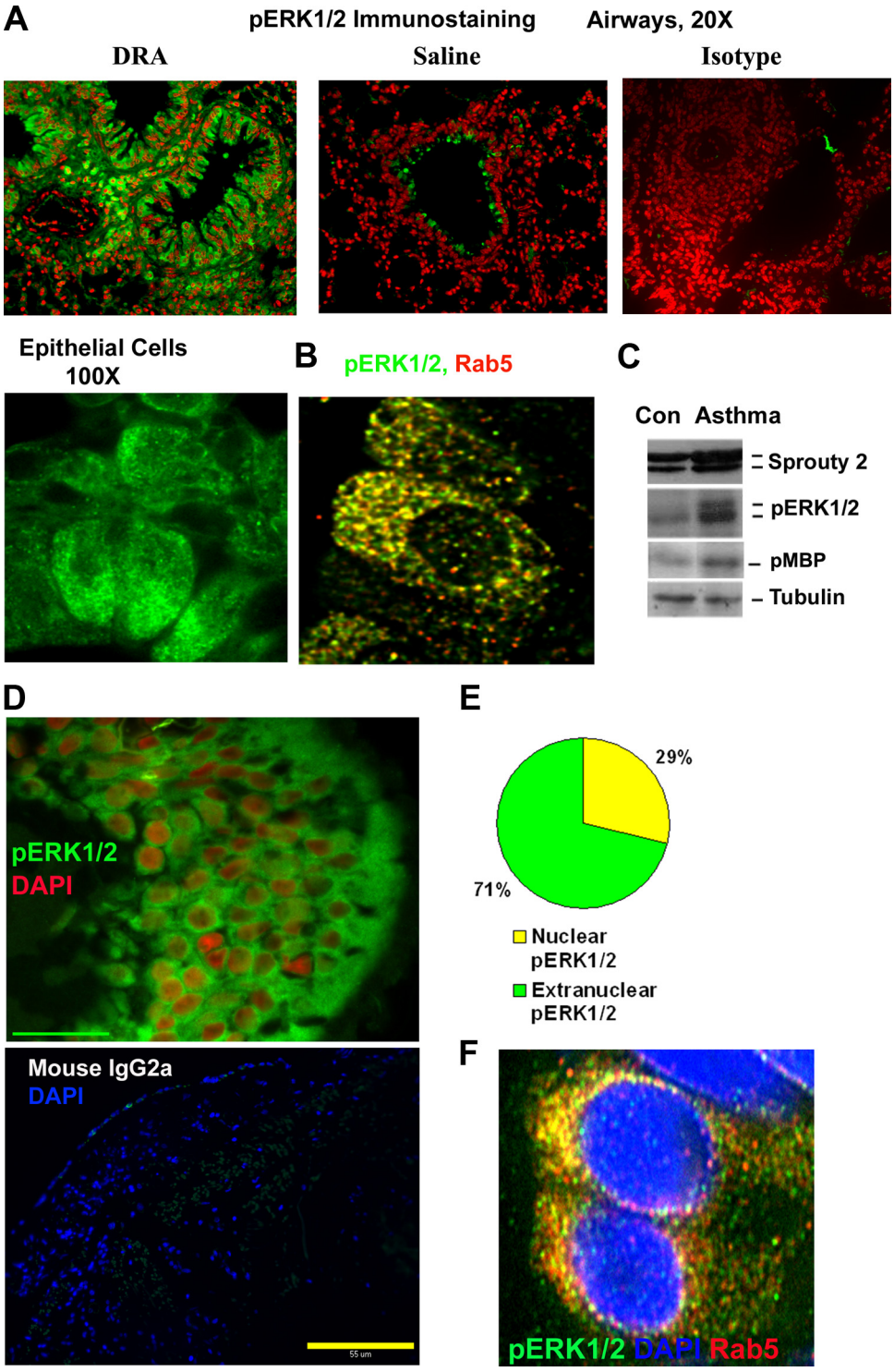

FIG. 10. Endosomal pERK1/2 in a mouse model of chronic asthma and human asthma. (A) Mice were immunized and exposed to a combination of three allergens, dust mites, ragweed, and *Aspergillus* (DRA), or saline as described previously (31). Three weeks after the last allergen exposure the mice were examined for pERK1/2 immunostaining (green). Nuclei were stained with DAPI and pseudocolored red for better visualization ($n = 6$). (B) Z-stack series of an airway epithelium stained with pERK1/2 (green) and Rab5 (red) were deconvolved by the software Metamorph, v.7, with point spread function. An overlay image showing colocalization in yellow is also shown ($n = 4$). (C) Lung tissue samples from the chronic asthma model (DRA sensitized and exposed) or control (Con; saline) were Western blotted for Sprouty 2 and pERK1/2 ($n = 3$). Another sample was immunoprecipitated with an anti-ERK1/2 antibody and used in the kinase assay in the presence of myelin basic protein (MBP) as a substrate ($n = 3$). (D to F) Endosomal pERK1/2 in human asthma. (D) Lung biopsy samples obtained from 6 asthmatic subjects were immunostained for pERK1/2 and counterstained with DAPI (pseudocolored red) as described previously (31). A representative airway epithelial image (magnification, $\times 100$) is shown. The lower panel shows immunostaining with an isotype control antibody. Scale bar = 55 μm. (E) Cells with nuclear staining for pERK1/2 from 100 epithelial cells per sample were counted, and the fraction of epithelial cells with nuclear pERK1/2 is presented ($n = 8$). (F) Selected biopsy samples were stained for pERK1/2 (green), Rab5 (red), and nuclei (DAPI; blue). Z-stack series were deconvolved by the software Metamorph, v.7, with point spread function. An overlay image showing colocalization in yellow is shown ($n = 4$).

airway hyperreactivity (11). The presence of hyperreactivity suggests that the airways are primed for heightened response to environmental stimuli. In this paper we show that, in asthma patients, the epithelial pERK1/2 is localized to $Rab5^+$ endosomes and that this endosomal localization promotes priming of epithelial cells. Experimental approaches and mathematical analyses of the Snl1 branch of the Hog1 MAPK pathway have shown that a system with high basal signaling exhibits higher efficiency, i.e., it shows a faster response time and higher sensitivity to variations in external signals (32). We speculate that the high basal activity of the endosomally localized pERK1/2 contributes to epithelial hyperreactivity. ERK1/2 has been shown to play a nonredundant role in IL-13 activation of airway epithelial cells (27).

Our signaling knowledge is primarily based upon signaling events that occur after a single stimulation of cells. In this paper we show that repeated stimulation of cells with the same ligand leads to a different outcome. Many hormones and other mediators are secreted in a rhythmic and cyclical manner. Even certain transcriptional events and chromatin remodeling follow a cyclical rhythm (22, 34). Our repeated stimulation mimics some of these cyclical processes. Thus, the results of our study have broader implications beyond IL-13 activation of epithelial cells. In summary, we have identified a mechanism of bistability in the ERK1/2 pathway that involves repeated stimulation with cytokines or growth factors and expression of Sprouty. We recognize that this may be only one of a number of mechanisms for achieving bistability.

ACKNOWLEDGMENTS

This work was supported by NIH grants RO1 AI059719 and AI68088, PPG HL 36577, and N01 HHSN272200700048C.

REFERENCES

1. **Bashor, C. J., N. C. Helman, S. Yan, and W. A. Lim.** 2008. Using engineered scaffold interactions to reshape MAP kinase pathway signaling dynamics. Science **319:**1539–1543.
2. **Bhattacharya, M., N. Ojha, S. Solanki, C. K. Mukhopadhyay, R. Madan, N. Patel, G. Krishnamurthy, S. Kumar, S. K. Basu, and A. Mukhopadhyay.** 2006. IL-6 and IL-12 specifically regulate the expression of Rab5 and Rab7 via distinct signaling pathways. EMBO J. **25:**2878–2888.
3. **Casci, T., J. Vinós, and M. Freeman.** 1999. Sprouty, an intracellular inhibitor of Ras signaling. Cell **96:**655–665.
4. **Chandramouli, S., C. Y. Yu, P. Yusoff, D. H. Lao, H. F. Leong, K. Mizuno, and G. R. Guy.** 2008. Tesk1 interacts with Spry2 to abrogate its inhibition of ERK phosphorylation downstream of receptor tyrosine kinase signaling. J. Biol. Chem. **283:**1679–1691.
5. **Das, J., M. Ho, J. Zikherman, C. Govern, M. Yang, A. Weiss, A. K. Chakraborty, and J. P. Roose.** 2009. Digital signaling and hysteresis characterize ras activation in lymphoid cells. Cell **136:**337–351.
6. **DaSilva, J., L. Xu, H. J. Kim, W. T. Miller, and D. Bar-Sagi.** 2006. Regulation of sprouty stability by Mnk1-dependent phosphorylation. Mol. Cell. Biol. **26:**1898–1907.
7. **Day, C. L., H. Puthalakath, G. Skea, A. Strasser, I. Barsukov, L. Y. Lian, D. C. Huang, and M. G. Hinds.** 2004. Localization of dynein light chains 1 and 2 and their pro-apoptotic ligands. Biochem. J. **377:**597–605.
8. **Edwin, F., R. Singh, R. Endersby, S. J. Baker, and T. B. Patel.** 2006. The tumor suppressor PTEN is necessary for human Sprouty 2-mediated inhibition of cell proliferation. J. Biol. Chem. **281:**4816–4822.
9. **Egan, J. E., A. B. Hall, B. A. Yatsula, and D. Bar-Sagi.** 2002. The bimodal regulation of epidermal growth factor signaling by human Sprouty proteins. Proc. Natl. Acad. Sci. U. S. A. **99:**6041–6046.
10. **Ferrell, J. E., and W. Xiong.** 2001. Bistability in cell signaling: how to make continuous processes discontinuous, and reversible processes irreversible. Chaos **11:**227–236.
11. **Fixman, E. D., A. Stewart, and J. G. Martin.** 2007. Basic mechanisms of development of airway structural changes in asthma. Eur. Respir. J. **29:**379–389.
12. **Formstecher, E., J. W. Ramos, M. Fauquet, D. A. Calderwood, J. C. Hsieh, B. Canton, X. T. Nguyen, J. V. Barnier, J. Camonis, M. H. Ginsberg, and H. Chneiweiss.** 2001. PEA-15 mediates cytoplasmic sequestration of ERK MAP kinase. Dev. Cell **1:**239–250.
13. **Goplen, N., M. Z. Karim, Q. Liang, M. M. Gorska, S. Rozario, L. Guo, and R. Alam.** 2009. Combined sensitization of mice to extracts of dust mite, ragweed, and Aspergillus species breaks through tolerance and establishes chronic features of asthma. J. Allergy Clin. Immunol. **123:**925–932.e11.
14. **Gorska, M. M., S. J. Stafford, O. Cen, S. Sur, and R. Alam.** 2004. Unc119, a novel activator of Lck/Fyn, is essential for T cell activation. J. Exp. Med. **199:**369–379.
15. **Hacohen, N., S. Kramer, D. Sutherland, Y. Hiromi, and M. A. Krasnow.** 1998. Sprouty encodes a novel antagonist of FGF signaling that patterns apical branching of the Drosophila airways. Cell **92:**253–263.
16. **Hall, A. B., N. Jura, J. DaSilva, Y. J. Jang, D. Gong, and D. Bar-Sagi.** 2003. hSpry2 is targeted to the ubiquitin-dependent proteasome pathway by c-Cbl. Curr. Biol. **13:**308–314.
17. **Hanafusa, H., S. Torii, T. Yasunaga, and E. Nishida.** 2002. Sprouty1 and Sprouty2 provide a control mechanism for the Ras/MAPK signalling pathway. Nat. Cell Biol. **4:**850–858.
18. **Hervagault, J. F., and S. Canu.** 1987. Bistability and irreversible transitions in a simple substrate cycle. J. Theor. Biol. **127:**439–449.
19. **Impagnatiello, M. A., S. Weitzer, G. Gannon, A. Compagni, M. Cotten, and G. Christofori.** 2001. Mammalian sprouty-1 and -2 are membrane-anchored phosphoprotein inhibitors of growth factor signaling in endothelial cells. J. Cell Biol. **152:**1087–1098.
20. **Inder, K., A. Harding, S. J. Plowman, M. R. Philips, R. G. Parton, and J. F. Hancock.** 2008. Activation of the MAPK module from different spatial locations generates distinct system outputs. Mol. Biol. Cell **19:**4776–4784.
21. **Jacquier, A., E. Buhler, M. K. Schäfer, D. Bohl, S. Blanchard, C. Beclin, and G. Haase.** 2006. Alsin/Rac1 signaling controls survival and growth of spinal motoneurons. Ann. Neurol. **60:**105–117.
22. **Kangaspeska, S., B. Stride, R. Métivier, M. Polycarpou-Schwarz, D. Ibberson, R. P. Carmouche, V. Benes, F. Gannon, and G. Reid.** 2008. Transient cyclical methylation of promoter DNA. Nature **452:**112–115.
23. **Kim, H. J., L. J. Taylor, and D. Bar-Sagi.** 2007. Spatial regulation of EGFR signaling by Sprouty2. Curr. Biol. **17:**455–461.
24. **Klein, O. D., G. Minowada, R. Peterkova, A. Kangas, B. D. Yu, H. Lesot, M. Peterka, J. Jernvall, and G. R. Martin.** 2006. Sprouty genes control diastema tooth development via bidirectional antagonism of epithelial-mesenchymal FGF signaling. Dev. Cell **11:**181–190.
25. **Kramer, S., M. Okabe, N. Hacohen, M. A. Krasnow, and Y. Hiromi.** 1999. Sprouty: a common antagonist of FGF and EGF signaling pathways in Drosophila. Development **126:**2515–2525.
26. **Lao, D. H., S. Chandramouli, P. Yusoff, C. W. Fong, T. Y. Saw, L. P. Tai, C. Y. Yu, H. F. Leong, and G. R. Guy.** 2006. A Src homology 3-binding sequence on the C terminus of Sprouty2 is necessary for inhibition of the Ras/ERK pathway downstream of fibroblast growth factor receptor stimulation. J. Biol. Chem. **281:**29993–30000.
27. **Lee, P. J., X. Zhang, P. Shan, B. Ma, C. G. Lee, R. J. Homer, Z. Zhu, M. Rincon, B. T. Mossman, and J. A. Elias.** 2006. ERK1/2 mitogen-activated protein kinase selectively mediates IL-13-induced lung inflammation and remodeling in vivo. J. Clin. Invest. **116:**163–173.
28. **Lin, J., A. Harding, E. Giurisato, and A. S. Shaw.** 2009. KSR1 modulates the sensitivity of mitogen-activated protein kinase pathway activation in T cells without altering fundamental system outputs. Mol. Cell. Biol. **29:**2082–2091.
29. **Lisman, J. E.** 1985. A mechanism for memory storage insensitive to molecular turnover: a bistable autophosphorylating kinase. Proc. Natl. Acad. Sci. U. S. A. **82:**3055–3057.
30. **Liu, W., Q. Liang, S. Balzar, S. Wenzel, M. Gorska, and R. Alam.** 2008. Cell-specific activation profile of extracellular signal-regulated kinase 1/2, Jun N-terminal kinase, and p38 mitogen-activated protein kinases in asthmatic airways. J. Allergy Clin. Immunol. **121:**893–902.e2.
31. **Lu, A., F. Tebar, B. Alvarez-Moya, C. López-Alcalá, M. Calvo, C. Enrich, N. Agell, T. Nakamura, M. Matsuda, and O. Bachs.** 2009. A clathrin-dependent pathway leads to KRas signaling on late endosomes en route to lysosomes. J. Cell Biol. **184:**863–879.
32. **Macia, J., S. Regot, T. Peeters, N. Conde, R. Solé, and F. Posas.** 2009. Dynamic signaling in the Hog1 MAPK pathway relies on high basal signal transduction. Sci. Signal. **2(63):**ra13.
33. **Markevich, N. I., J. B. Hoek, and B. N. Kholodenko.** 2004. Signaling switches and bistability arising from multisite phosphorylation in protein kinase cascades. J. Cell Biol. **164:**353–359.
34. **Métivier, R., G. Penot, M. R. Hübner, G. Reid, H. Brand, M. Kos, and F. Gannon.** 2003. Estrogen receptor-alpha directs ordered, cyclical, and combinatorial recruitment of cofactors on a natural target promoter. Cell **115:**751–763.
35. **Moarefi, I., M. LaFevre-Bernt, F. Sicheri, M. Huse, C. H. Lee, J. Kuriyan, and W. T. Miller.** 1997. Activation of the Src-family tyrosine kinase Hck by SH3 domain displacement. Nature **385:**650–653.
36. **Nadeau, R. J., J. L. Toher, X. Yang, D. Kovalenko, and R. Friesel.** 2007. Regulation of Sprouty2 stability by mammalian Seven-in-Absentia homolog 2. J. Cell. Biochem. **100:**151–160.
37. **Nechamen, C. A., R. M. Thomas, and J. A. Dias.** 2007. APPL1, APPL2, Akt2

and FOXO1a interact with FSHR in a potential signaling complex. Mol. Cell. Endocrinol. **260–262:**93–99.

38. **Qui, M., and S. Green.** 1992. PC12 cell neuronal differentiation is associated with prolonged p21ras activity and consequent prolonged ERK activity. Neuron **9:**705–717.
39. **Rao, N., I. Dodge, and H. Band.** 2002. The Cbl family of ubiquitin ligases: critical negative regulators of tyrosine kinase signaling in the immune system. J. Leukoc. Biol. **71:**753–763.
40. **Romero Rosales, K., E. R. Peralta, G. G. Guenther, S. Y. Wong, and A. L. Edinger.** 2009. Rab7 activation by growth factor withdrawal contributes to the induction of apoptosis. Mol. Biol. Cell **20:**2831–2840.
41. **Rubin, C., V. Litvak, H. Medvedovsky, Y. Zwang, S. Lev, and Y. Yarden.** 2003. Sprouty fine-tunes EGF signaling through interlinked positive and negative feedback loops. Curr. Biol. **13:**297–307.
42. **Rubin, C., Y. Zwang, N. Vaisman, D. Ron, and Y. Yarden.** 2005. Phosphorylation of carboxyl-terminal tyrosines modulates the specificity of Sprouty-2 inhibition of different signaling pathways. J. Biol. Chem. **280:**9735–9744.
43. **Schenck, A., L. Goto-Silva, C. Collinet, M. Rhinn, A. Giner, B. Habermann, M. Brand, and M. Zerial.** 2008. The endosomal protein Appl1 mediates Akt substrate specificity and cell survival in vertebrate development. Cell **133:** 486–497.
44. **Tefft, D., M. Lee, S. Smith, D. L. Crowe, S. Bellusci, and D. Warburton.** 2002. mSprouty2 inhibits FGF10-activated MAP kinase by differentially binding to upstream target proteins. Am. J. Physiol. Lung Cell. Mol. Physiol. **283:**L700–L706.
45. **Tian, T., A. Harding, K. Inder, S. Plowman, R. G. Parton, and J. F. Hancock.** 2007. Plasma membrane nanoswitches generate high-fidelity Ras signal transduction. Nat. Cell Biol. **9:**905–914.
46. **Topp, J. D., N. W. Gray, R. D. Gerard, and B. F. Horazdovsky.** 2004. Alsin is a Rab5 and Rac1 guanine nucleotide exchange factor. J. Biol. Chem. **279:**24612–24623.
47. **Traverse, S., N. Gomez, H. Paterson, C. Marshall, and P. Cohen.** 1992. Sustained activation of the mitogen-activated protein (MAP) kinase cascade may be required for differentiation of PC12 cells. Comparison of the effects of nerve growth factor and epidermal growth factor. Biochem. J. **288:**351–355.
48. **Tresini, M., A. Lorenzini, C. Torres, and V. J. Cristofalo.** 2007. Modulation of replicative senescence of diploid human cells by nuclear ERK signaling. J. Biol. Chem. **282:**4136–4151.
49. **Valdembri, D., P. T. Caswell, K. I. Anderson, J. P. Schwarz, I. König, E. Astanina, F. Caccavari, J. C. Norman, M. J. Humphries, F. Bussolino, and G. Serini.** 2009. Neuropilin-1/GIPC1 signaling regulates alpha5beta1 integrin traffic and function in endothelial cells. PLoS Biol. **7:**e25.
50. **Wang, J., W. H. Shen, Y. J. Jin, P. W. Brandt-Rauf, and Y. Yin.** 2007. A molecular link between E2F-1 and the MAPK cascade. J. Biol. Chem. **282:** 18521–18531.
51. **Wills-Karp, M., and F. D. Finkelman.** 2008. Untangling the complex web of IL-4- and IL-13-mediated signaling pathways. Sci. Signal. **1:**pe55.
52. **Wong, E. S., C. W. Fong, J. Lim, P. Yusoff, B. C. Low, W. Y. Langdon, and G. R. Guy.** 2002. Sprouty2 attenuates epidermal growth factor receptor ubiquitylation and endocytosis, and consequently enhances Ras/ERK signalling. EMBO J. **21:**4796–4808.
53. **Xiong, W., and J. E. Ferrell Jr.** 2003. A positive-feedback-based bistable 'memory module' that governs a cell fate decision. Nature **426:**460–465.
54. **Yigzaw, Y., H. M. Poppleton, N. Sreejayan, A. Hassid, and T. B. Patel.** 2003. Protein-tyrosine phosphatase-1B (PTP1B) mediates the anti-migratory actions of Sprouty. J. Biol. Chem. **278:**284–288.
55. **Yildirim, N., M. Santillan, D. Horike, and M. C. Mackey.** 2004. Dynamics and bistability in a reduced model of the lac operon. Chaos **14:**279–292.